DEMO INTERIM STRUCTURAL DESIGN CRITERIA

DISDC

APPENDIX A MATERIAL DESIGN LIMIT DATA

A3.S18E EUROFER STEEL

DRAFT

INTERIM TTMS 5.2 & 5.5 REPORTS

F. TAVASSOLI

CEA/DEN/SAC/DMN

D0 – 155 – 21/06/02

Revision 0

Dec. 2002

Commissariat à l'Energie Atomique

CEA/Saclay, DMN/Dir, 91191 Gif sur Yvette cedex, France

July 2002

Table of contents

A3.S18E.4.5 Irradiation Induced Creep Curve (ϕt_{c1}) for the Test to Determine if Nonlinear Analysis is Needed

A3.S18E.4.6 Negligible irradiation induced creep curve

A3.S18E.5 ANALYSIS DATA

A3.S18E.5.1 Values of S_m

A3.S18E.5.2 Values of S_t

A3.S18E.5.3 Values of S_r

A3.S18E.5.4 Fatigue Curves at Saturation

A3.S18E.5.5 Isochronus and Creep Deformation Curves

A3.S18E.5.6 Values of S_{Rh} and S_{Rc}

A3.S18E.5.7 Symetrisation Factor, K_s

A3.S18E.5.8 Creep-Fatigue Interaction Diagram

A3.S18E.5.9 Cyclic Curves, Values of K_ε and K_ν

A3.S18E.6 ADDITIONAL ANALYSES

A3.S18E.6.1 Monotonic Hardening Curve in Tension

A3.S18E.6.2 Bilinear Curves

A3.S18E.6.3 Creep Deformation Curve

A3.S18E.6.4 Fatigue Curves

A3.S18E.6.5 Maximum allowable damage: D_{max}

ACKNOWLEDGEMENTS

The results used in this work come from the European RAFM database that is still expanding. Several American, Russian and Japanese institutes have also contributed to this database. The main European contributing institutes to the Eurofer data base and their investigators are:

- CEA/SRMA: A. Alamo, A. Bougault, Y. De Carlan, C.A. Danon, S. Urvoy
- CEA/STA: A. Fontes, L. Forest
- CEA/SGM: L. Bedel, I. Chu, J-M. Gentzbittel, P. Lemoine, B. Riccetti, E. Rigal,
- CIEMAT: P. Fernãndez, A-M. Lancha, J. Lapeña,
- CRPP: N. Baluc, Marmy, P. Spätig, M. Victoria,
- ENEA: G. Filacchioni, C. Fazio, ?),
- FZK/IMF: E. Diegele, K. Ehrlich, R. Lindau, A. Möslang, K. Petersen, Schaefer, M. Schirra, R. Schmitt, ?, ?),
- NRG: B. van der Schaaf, J-W. Rensman, E.W. Schuring, H.E. Hofmans
- NFR (S. Tähtinen),
- RISOE: B.N. Singh,
- SCK (E. Lucon),
- VTT (A. Lind);
- N.C.S.R. "Demokritos": K. Mergia, M. Messoloras, …
- EFDA-CSU: M. Gasparotto, G. Le Marois

Principal documents consulted are:

1. R. Lindau, communication to EU partners
2. M. Schirra A. Falkenstein, P. Graf, S. Heger, H. Kempe, R. Lindau, H. Zimmermann, FZKA 6707, April 2002
3. IEA Sponsored workshops on ferritic/martensitic steel proceedings covering data from Europe, Japan and US.
4. H.E. Hofmans, NRG 20023/00.38153/P, Petten, 15 Dec. 2000
5. A. Alamo, et al, NT SRMA 2001-2419.
6. Boehler Certificates issued for Eurofer fabrication.
7. A.M. Lancha, P. Fernandez, CIEMAT, private communications.

8. E. Lucon, A. Leenaers, SCK/Mol, Mechanical Characterization of EUROFER97 Irradiated to 0.32 dpa at 300 °C, March 2002

9. G. Filacchioni, The Thermo-Mechanical Fatigue Testing Facility of Casaccia's Laboratories, MAT-TEC, March 2002

A3.S18E.1 MATERIALS

A3.S18E.1.1 Introduction

This document follows the Appendix A: GEN, where the definitions of the physical and mechanical properties used in the ISDC together with the formulae used in calculating various design limits are presented. It also follows the Appendices A3.S18 and A3.S18F, where materials properties data and design values are reported respectively for the conventional Mod. 9Cr-1Mo steel and F82H steel, a Reduced Activation Ferritic / Martensitic steel (RAFM).

The Eurofer steel is also an RAFM steel. It is produced in Europe as compared with F82H, which is produced in Japan. Both alloys development efforts are integrated in the IEA Fusion Materials implementing agreement, where US, RF, Japan, China and EU are active partners.

Notice: Due to the fact that characterization of the Eurofer steel is still in progress, the results presented here are tentative and subject to revisions in future editions of Appendix A3.S18E.

A3.S18E.1.2 Products and Compositions

Several 2000 kg heats of Eurofer steel (designated Eurofer 97) have been produced for EU by Böhler / Austria (production No. T512) to the specification provided in Table 1.2.1. Drawings of the items delivered are given in Annex 1 and their chemical compositions in Annex 2.

In the course of Eurofer 97 production, initial trial heats were remelted. 4 melts changed their initial names after remelting, one did not:

D83350 = E83350, D82117 = E83694, D82118 = E83697, D82119 = E83698, D82120 = E83699

The denominations retained hereafter are those beginning with E.

These heats have been shaped into plates, bars, tubes, wires and dispatched to several EU laboratories, see Annex 2..

All products are delivered by the manufacturer in normalised and tempered conditions (Böhler Certificate 200556, dated 02/11/1999).

The plates treatments are:

- 980°C/ 27 min/ air for items 10, 20
- 980 °C/ 30.6 min/air for items 30, 40
- Temper of all items (10-40) at 760 °C/ 90 min /air.

The forged bars (E83699) treatments are:

- 979 °C / 1 h 51 min. /air cooled
- 739 °C / 3 h 42 min. /air cooled

Plates are grouped by the manufacturer in four items:

- Item 10 covers lot number 248 from Heat E83698, it includes two 8 mm plates (No. 66 & 77) cut into 22 smaller plates and numbered 66/1 through 66/12 and 77/1 through 77/10.

- Item 20 covers lot number 249 from Heat E83698, it includes two 14 mm plates (No. 3 & 4) cut into 27 smaller plates and numbered 3/1 through 3/12 and 4/1 through 4/15.

- Item 30 covers lot number 251 from Heat E83694, it includes a 25 mm plate (No. 1) cut into 15 smaller plates: 1/1 through 1/15. Item 30 also covers lot number 250 from Heat E83697, it includes a 25 mm plate (No. 2) cut into 15 smaller plates and numbered 2/1 through 2/15.

- Item 40 covers lot number 247 from Heat E83698, it includes two 1.5 mm plates (No. 1 & 2) cut into 24 smaller plates and numbered 1/1 through 1/12 and 2/1 through 2/12.

From the heat E83350, tubes (10x1, 17x1.5, 13.5x1.25 mm) and wire (1 mm) are produced.

Six bars are produced from E83699 forged bar.

All products are fully martensitic and have grain sizes of 9 for lots 248, 249, 250, 251 and 10 for lot 247 and forged bars (E83699), see Annex 3.

TIG welded joints of Eurofer 97 are produced with matching filler material (1 mm wire). The operating conditions used are similar to those employed for F82H steel (U= 10 V, I= 150-230 A, welding speed = 4 cm/min, wire speed = 0.7 – 2 mm/min, scanning width = 3.5 – 9.5 mm). Welded joints are post weld heat treated.

Solid HIP joints are made at CEA/Grenoble from the end of 100 mm S-S6 bar (heat E8699), see Annex 4. For this purpose disk slices are cut from the bar. They are machined to Ra 0.8 µm and degreased with the container in a mixture of alcohol , ether and acetone in an ultrasonic bath. Then rinsed with alcohol and dried. After placing the slices in the container, they are degassed at 60 °C for 15 h before sealing under argon. The HIP cycle takes 2 h to reach temperature of 1100 °C and pressure of 100 MPa, where it is maintained for 2 h, and then cooled down for another 2 h to room temperature. A post bond heat treatment is applied to the joint:

- first the joint is heated to 750 °C and maintained for 1 h,

- then the temperature is increased to 950 °C, held for 1 h, followed by air cooling.

- The final temper is carried out at 750 °C for 1 h.

Powder HIP products are produced from atomising the Eurofer product. Particles of medium size (45µm < d < 250 µm) are HIPed at 1040 °C, for 4 hours under a pressure of 140 MPa. Due to large size of the HIP product (ø 67, l = 110mm) and slow cooling, a post HIP normalising is applied :

- 980 °C / 1 h water cooled,

- followed by temper at 750 °C for 2 h.

HIP products are marked E1, E2, and so on.

Elements	F82H Steel	Eurofer 97 Steel
Cr	7.7	8,5 - 9,5 [9.0]
C	0.09	0.09 – 0.12 [0.11]
Mn	0.16	0.20 – 0.60 [0.40]
P	0.002	< 0.005
S	0.002	< 0.005
V	0.16	0.15 – 0.25
B	0.0002	< 0,001
N2	0.006	0.015 – 0.045 [0.030]
O2	(0.01)	< 0,01
W	1.94	1.0 - 1.2 [1.1]
Ta	0.02	0.06 - 0.09
Ti	100 ppm	< 0.01 (100 ppm)
Nb	1 ppm	[<10 ppm]
Mo	30 ppm	[< 50 ppm]
Ni	200 ppm	[< 50 ppm]
Cu	100 ppm	[< 50 ppm]
Al	30 ppm	[<100 ppm]
Si	1100 ppm	< 500 ppm
Co	50 ppm	[< 50 ppm]
Sn	(< 20 ppm)	As+Sn+Sb+Zr < 100 ppm
As	(< 50 ppm)	As+Sn+Sb+Zr < 100 ppm

Table A3.S18E.1.2.1. Specified compositions for Eurofer 97 in wt%, unless otherwise stated. Those of F82H steel are also given for comparison. (Target values in [ ]).

A3.S18E.1.3 Quality Safe Guarding Data:

Specifications for quality safe guarding are not available as yet for Eurofer steel. As an interim step those of the conventional Mod. 9Cr-1Mo steel (A3.S18) are used.

	20°C (plate)	20°C (tubes)	550°C
Yield stress, S_y	> 400 MPa	> 420 MPa	>260 MPa
Ultimate Tensile Strength, S_u	580-700 MPa	580-700 MPa	>260 MPa
Total Elongation over 5d	> 20%		

°C (plate)	KCV (daJ/cm^2)
0	7.0 (mean) 5.0 (min)
-20	5.0 (mean) 3.5 (min)
+20	9.0 (min)

Table A3.S18E.1.3.1. Interim recommendations for quality safe guarding.

(values given are those of A3.S18)

A3.S18E.2 PHYSICAL PROPERTIES

A3.S18E.2.1 Coefficient of Thermal Expansion

a. Unirradiated condition

Average values (α_m) are not available yet for Eurofer steel, those of F82H steel are used. Those of F82H are given by formula 2.1.1 and table 2.1.1. Instantaneous values of (α_i) reported by ENEA are slightly higher and are also given in table 2.1.1

- Formula 2.1.1

$$\alpha_m = 9.0955 + 4.6477 \text{ x}10^{-3}\ T - 1.2141 \text{ x}10^{-6}\ T^2 \qquad \text{(valid up to 800 °C)}$$

(α in 10^{-6}/K, T in K)

The average coefficient of linear thermal expansion α_m between room temperature and the considered temperature is given in table 2.11, and plotted in figure 2.11 (data source JAERI).

Temp. (C)	100	200	300	400	500	600	700	800	900	1000
α_m (10^{-6}/K)	10.7	11	11.2	11.7	12	12.3	12.5	12.6	10	10.7
α_i (10^{-6}/K)	11.7	12.3	12.8	13.3	13.9	14.4	14.9			

Table A3.S18E.2.1.1. Mean α_m (reference temperature = 20°C) coefficients of linear thermal expansion (on heating) of F82H (JAERI) and instantaneous α_i (ENEA) .

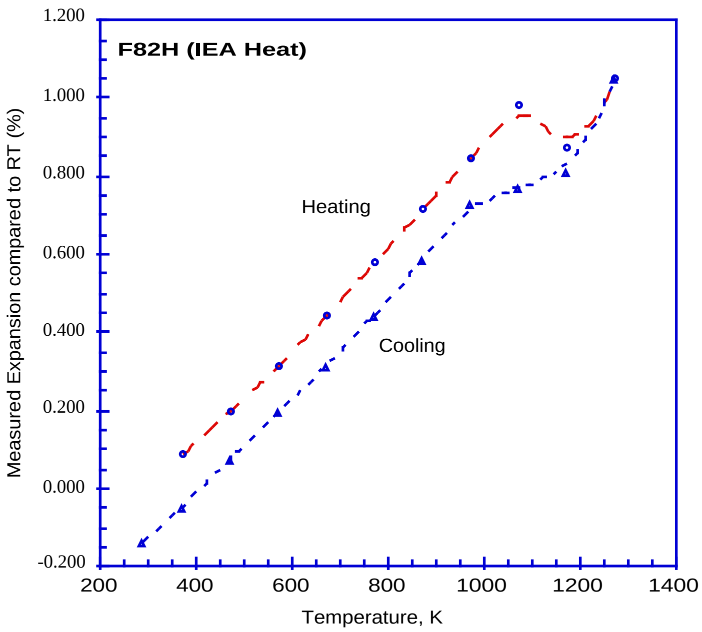

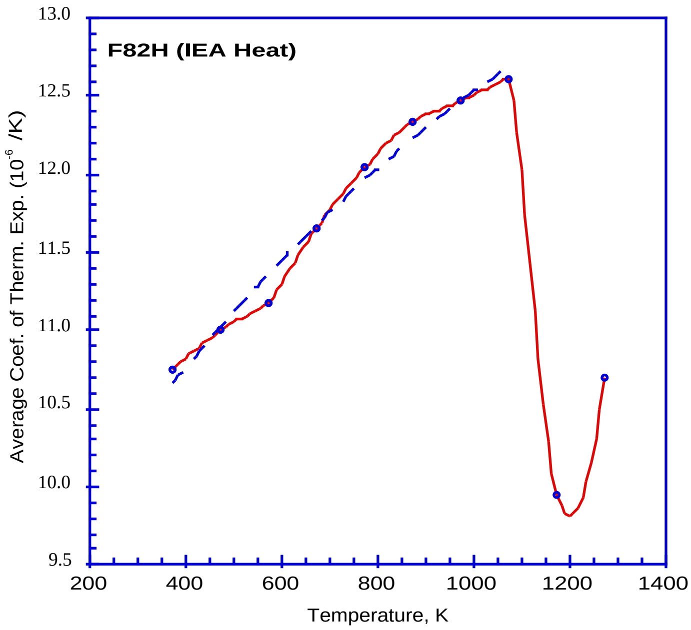

Figure A3.S18E.2.1.1. Mean coefficient of linear thermal expansion versus temperature.

b. Irradiated condition

Insufficient data available. The unirradiated values shall be used.

A3.S18E.2.2 Elastic and Regidity Moduli: E and G

a. Unirradiated condition

- Formulae 2.2.1 and 2.2.2

Dynamic values are not yet available for Eurofer steel, those of F82H steel are used. Variations of the modulus of elasticity (E) and Shear (G) are given as a function of the temperature θ (C) by the following equations.

$$E = 218.76 - 0.077834\ \theta + 1.4735\ \text{x}10^{-4}\ \theta^2 - 2.1998\ \text{x}10^{-7}\ \theta^3 \qquad (20\ °C \leq \theta \leq 700\ °C)$$

$$G = 84.902 - 0.03378\ \theta + 6.8965\ \text{x}10^{-5}\ \theta^2 - 9.828\ \text{x}10^{-8}\ \theta^3 \qquad (20\ °C \leq \theta \leq 700\ °C)$$

Where E and G are in GPa, θ in C. Values of E and G between RT and 700 C are given in table 2.2.1 and plotted in figure 2.2.1. Static values of modulus measured from tension curves for Eurofer in L orientation are also given. These values are approximate, have a large scatter (Figure 2.2.2) and are lower than the dynamics, also procedures for measuring static modulus are different from those of the tensile tests.

- Table 2.2.1

θ (C)	20	50	100	150	200	250	300	350	400	450	500	550	600	650	700
G (GPa)	84	83	82	81	80	79	78	77	76	75	73	71	68	65	61
E (GPa)	217	215	212	210	207	205	203	200	197	194	189	184	178	170	161
E (GPa) (tensile)	32.7			32.6			38.0			40.8	34.3	31.2	23.0	21.6	12.6

Table A3.S18E.2.2.1. Values of Elastic (E) and Rigidity (G) moduli from room temperature to 700 C for F82H and Static tensile (L) for Eurofer steel.

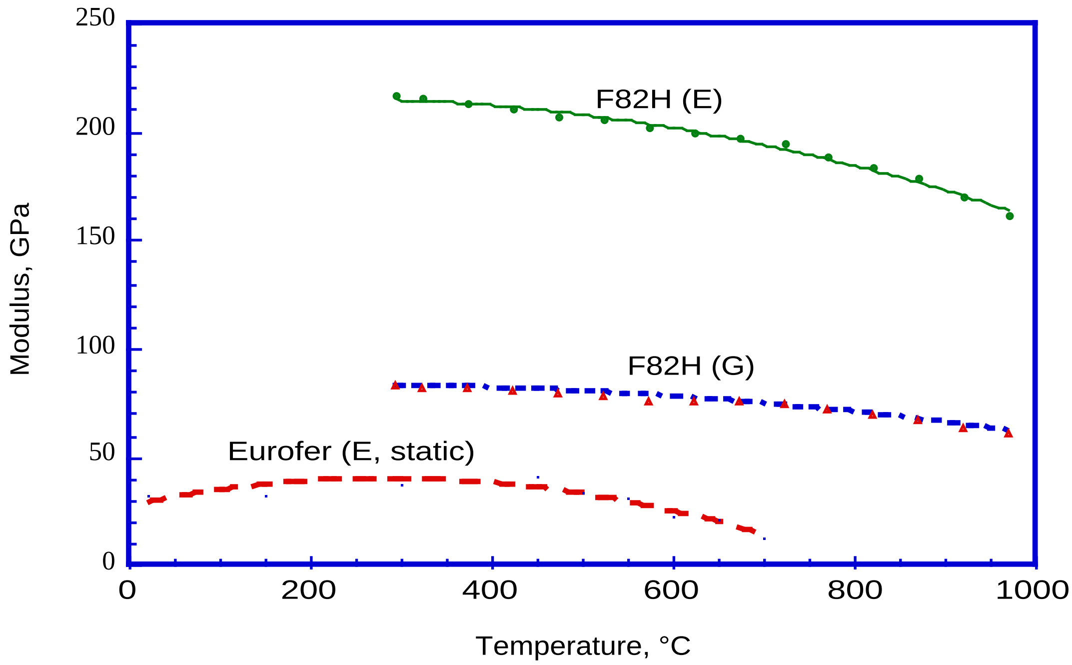

Figure A3.S18E.2.2.1. Elastic (E) and Regidity (G) moduli (JAERI experimental data shown in figure), and Eurofer E from tension tests.

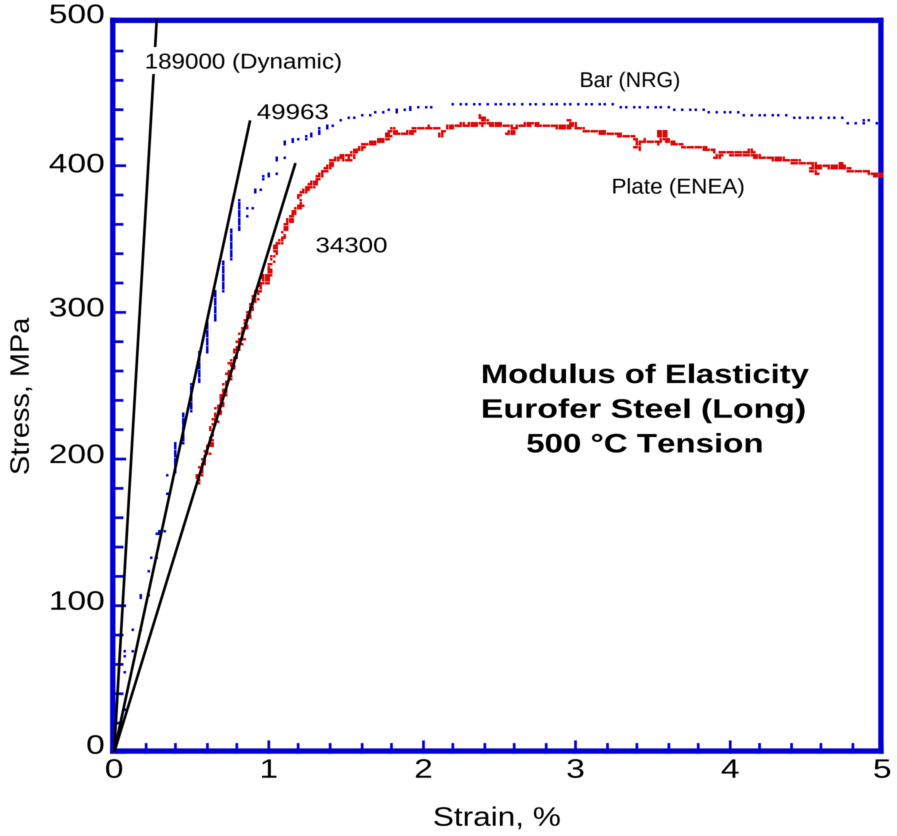

Figure A3.S18E.2.2.2. Comparison of slope of elastic section of tension curve (Eurofer), with dynamic slope deduced from dynamic value of E reported for F82H.

b. Irradiated condition

Modulus of elasticity is an inherent physical property of material. The unirradiated values shall be used in irradiated conditions. Effects of a reduction in effective cross section or of internal stresses should be accounted for under other topics.

A3.S18E.2.3 Poisson's Ratio: ν

An average value of 0.3 is assumed.

A3.S18E.2.4 Density: ρ

a. Unirradiated condition

- Formula 2.4.1

Not yet available for Eurofer steel yet, those of F82H steel are used.

Density of F82H at 20°C is 7870 kg/m^3. That of the Eurofer should be slightly lower. Assuming that the trend at temperature is similar to that of Mod. 9Cr-1Mo steel, the following tentative equation is derived using room temperature value of FH2H:

$$\rho = 7876.31 - 0.26576\,\theta - 11.216 \times 10^{-5}\,\theta^2$$

- Table 2.4.1

Values of ρ between RT and 600°C are given in table A3.S18E.2.4.1 and plotted in figure 2.4.1:

(°C)	20	100	200	300	400	500	600
ρ (kg/m3)	7871	7849	7819	7786	7752	7715	7676

Table A3.S18E.2.4.1. Extrapolated values of density from room temperature to 600°C.

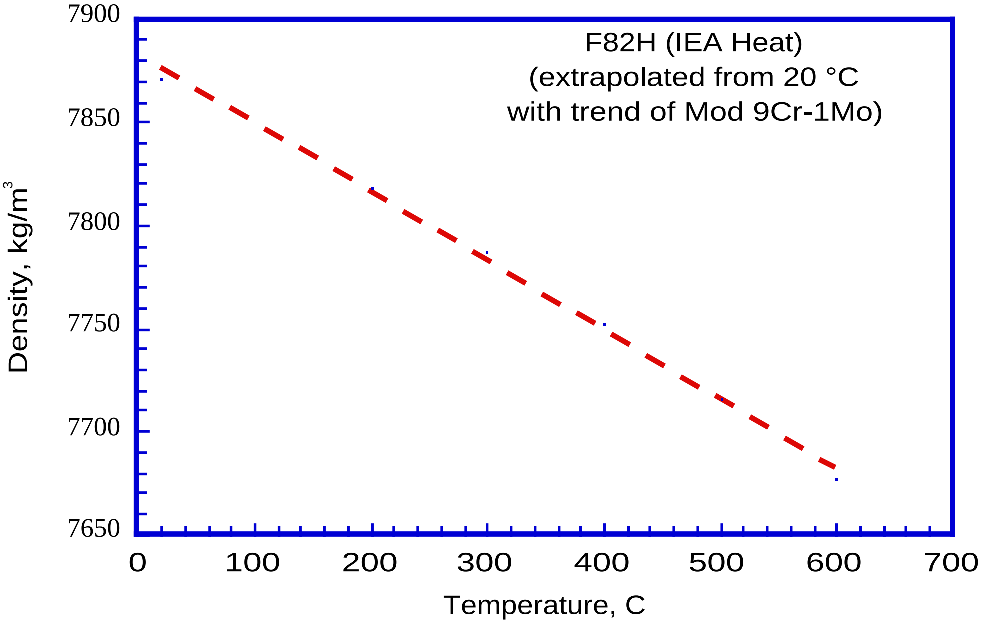

Figure A3.S18E.2.4.1. Tentative presentation of variation of density of F82H steel versus temperature (values at θ greater than 20°C are extrapolated values).

<u>b. Irradiated condition</u>

Irradiation has an effect on the density of materials through the formation of vacancies, voids and cavities. The effect of irradiation on the density is considered through the swelling law.

A3.S18E.2.5 Specific Heat, Thermal Conductivity, Thermal Diffusivity: C_p, k, and a

- Formulae 2.5.1-2.5.3

Not yet available for Eurofer steel, those of F82H steel are used. The equations describing variations of the specific heat (C_p), thermal conductivity (k), and thermal diffusivity (a) as a function of test temperature are given below (validity up to about 870 C):

(T in K)

$$C_p = 1390.2 - 7.8498\ T + 0.022969\ T^2 - 2.7446 \times 10^{-5}\ T^3 + 1.1932 \times 10^{-8}\ T^4$$

$$k = 28.384 - 0.011777\ T - 1.0632 \times 10^{-6}\ T^2 - 8.2935 \times 10^{-9}\ T^3$$

$$a = 0.089188 + 1.4051 \times 10^{-5}\ T - 5.7859 \times 10^{-8}\ T^2$$

- Table 2.51

Measured values of C_p , a , and k at temperatures RT to 800 C for F82H steel are given in table 2.5.1 and plotted in figures 2.5.1-2.5.3:

Temp. C	Specific Heat C_p (J/kg.K)	Thermal Diffusion Coef. a ($10^{-6}m^2/s$)	Thermal Conductivity k (W/m.K)
20	448	0.0885	31.3
50	460		
100	477	0.0865	32.5
150	494		
200	510	0.0822	32.9
250	527		
300	544	0.0785	33.4
350	565		
400	586	0.0725	33.0
450	611		
500	644	0.0656	32.7
550	682		
600	728	0.0575	32.3
650	782		
700	866	0.0479	31.9
750	1075		
760	1155		
800	803	0.0474	29.2

Table A3.S18E.2.5.1. Values of specific heat, thermal conductivity and thermal diffusivity for F82H steel, (JAERI data).

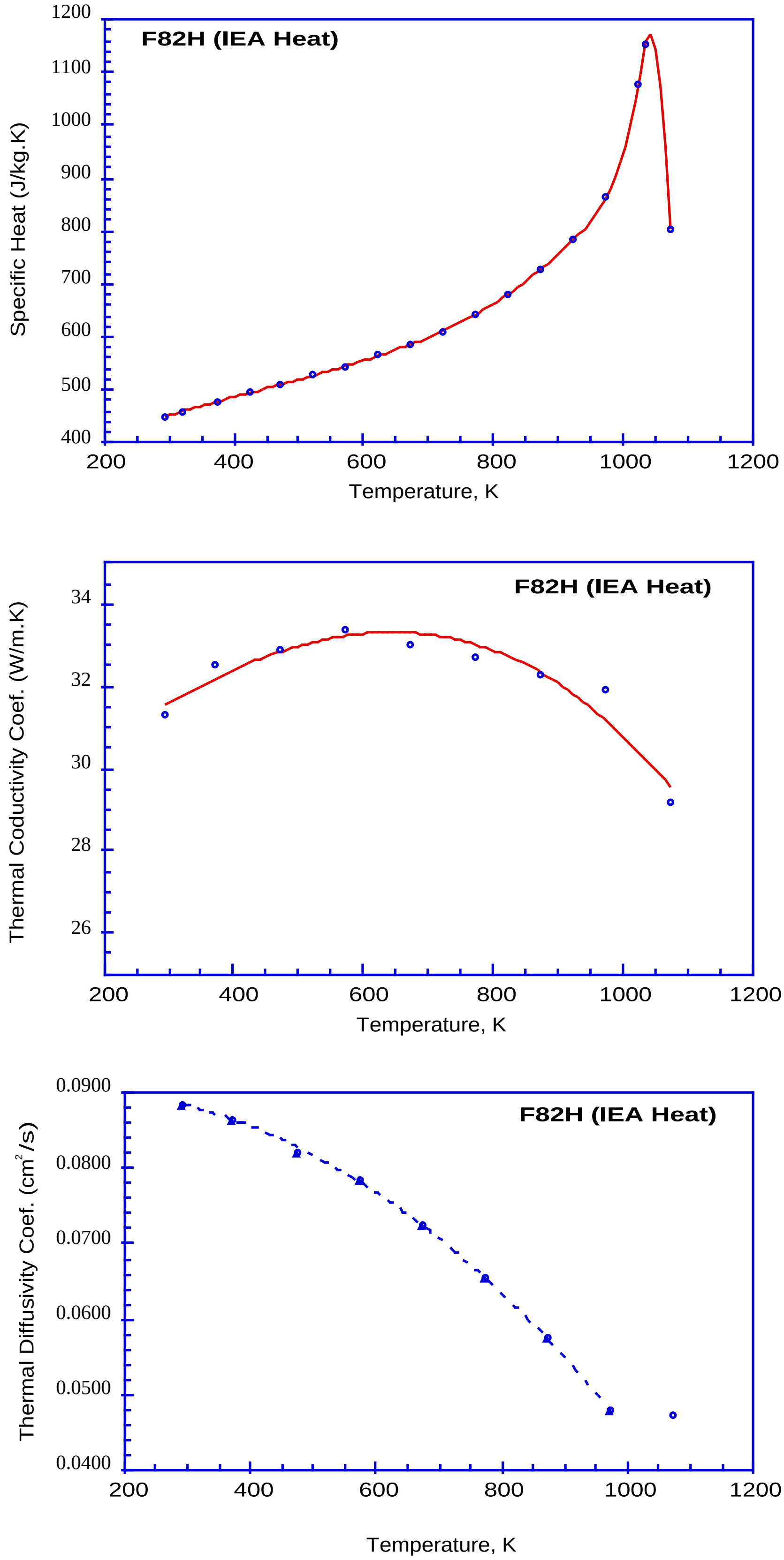

Figure A3.S18E.2.5.1 to 3. Specific heat, Thermal Conductivity, Thermal Diffusivity JAERI data).

A3.S18.2.6 Electrical Resistivity: Ω

a. Unirradiated condition

Not yet available for Eurofer steel, those of the conventional Mod. 9 Cr steel are used. Table A3.S18E.2.6.1, shows values of electrical resistivity (10^{-6} ohm.m) collected for grade 91 steel, at temperatures from room temperature up to 650°C.

Temp(°C)	20	50	100	150	200	250	300
(10^{-6}ohm.m)	0.502	0.526	0.564	0.603	0.642	0.682	0.722
Temp(°C)	350	400	450	500	550	600	650
(10^{-6}ohm.m)	0.763	0.803	0.844	0.886	0.927	0.968	1.010

Table A3.S18E.2.6.1. Interim electrical resistivity (grade 91 data) at various temperatures.

b. Irradiated condition

Not available

A3.S18E.2.7 Magnetic Properties

a. Unirradiated condition

Not yet available for Eurofer steel, those of F82H steel are used.

T (K)	File	Mass (kg)	σ (EMU/g)	H_{max} (Oe)	B_s (Gauss)	B_r (Gauss)	S_q	S* (A/Hc)	H_c (Oe)	ΔH (Oe)	Std (dH/Hc)
300	RTL	0.161	1.983E+2	1.500E+2	1.967E+4	2.162E+2	1.100E-2	4.496E-2	1.462E+1	2.264E+3	1.549E+2
	RTC	0170	1.960E+2	1.500E+2	1.943E+4	2.009E+2	1.034E-2	1.659E-2	1.473E+1	2.549E+3	1.731E+2
473	200L	0.161	1.910E+2	1.500E+2	1.894E+4	2.080E+2	1.098E-2	4.067E-2	1.372E+1	2.235E+3	1.629E+2
	200C1	0170	1.881E+2	1.500E+2	1.866E+4	1.931E+2	1.035E-2	2.941E-2	1.417E+1	2.452E+3	1.731E+2
573	300L	0.161	1.848E+2	1.500E+2	1.833E+4	1.895E+2	1.034E-2	1.672E-2	1.278E+1	2.160E+3	1.691E+2
	300C	0170	1.822E+2	1.500E+2	1.807E+4	1.697E+2	9.388E-3	3.333E-2	1.250E+1	2.367E+3	1.893E+2
673	400L	0.161	1.765E+2	1.500E+2	1.750E+4	1.668E+2	9.533E-3	6.216E-2	1.115E+1	2.060E+3	1.847E+2
	400C	0170	1.740E+2	1.500E+2	1.726E+4	1.697E+2	9.830E-3	-1.214E-2	1.214E+1	2.233E+3	1.839E+2

Table A3.S18E.2.7.1. Summary of F82H steel magnetic properties (source JAERI).

b. Irradiated condition

Not available

A3.S18E.2.8 Hardness

a. Unirradiated condition

Table A3.S18E.2.8.1 presents typical hardness values.

Roll No.	Plate No	Thickness (mm)	Average of 3 (HV10)
E83698	66	8	218-221
E83698	3	14	208-216
E83694	1	25	216-221
E83697	2	25	221-222
E83698	1	1.5	204
E83699		Ø 100	220

Table A3.S18E.2.8.1. Hardness of Eurofer products (Boehler data).

b. Irradiated condition

Varies with irradiation dose.

A3.S18E.3 TENSILE STRENGTH PROPERTIES

A3.S18E.3.1 Minimum and Average Yield Strength at 0.2 % Offset: S_y

a. Unirradiated conditions

Yield stress values obtained from tension tests performed on specimens cut in the longitudinal orientation of the 8, 14, and 25 mm plates and 100 mm bar are shown in Figure 3.1.

- Formulae 3.1.1 and 3.1.2

A third degree polynomial equation is fitted to figure 3.1. data. The mean S_y value at RT (20-27 °C) is 542.42 MPa, with a standard deviation of 14.972 MPa. This information is used to derive the minimum curve, i.e. applying a reduction coefficient of $(S_{y\ av} - 1.96 \text{ x SD}) / S_{y\ av} = 0.945$ to higher temperature results.

$$S_{y\ (av)} = 559.18 - 0.7267\ \theta + 2.3737 \cdot 10^{-3}\ \theta^2 - 3.1452 \times 10^{-6}\ \theta^3$$

$$S_{y\ (min)} = 0.945 \cdot (559.18 - 0.7267\ \theta + 2.3737 \cdot 10^{-3}\ \theta^2 - 3.1452 \times 10^{-6}\ \theta^3)$$

The above equations are valid in the range of 20°C < θ < 700°C.

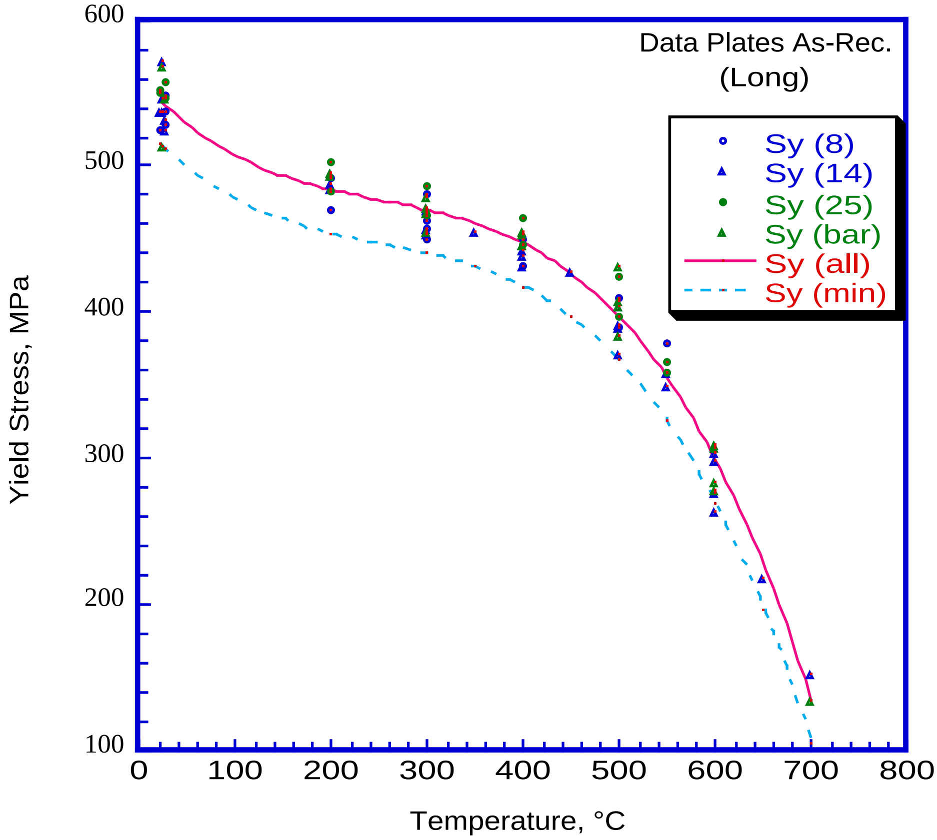

Figure A3.S18E.3.1.1. Yield stress (S_y) of Eurofer base metal plates and bars in longitudinal orientation versus test temperature (CEA, CIEMAT, FZK, NRG data).

The average and minimum curves obtained are adequately representative of the results obtained from tests on specimens taken in the transverse orientation of plates or radial direction of bars.

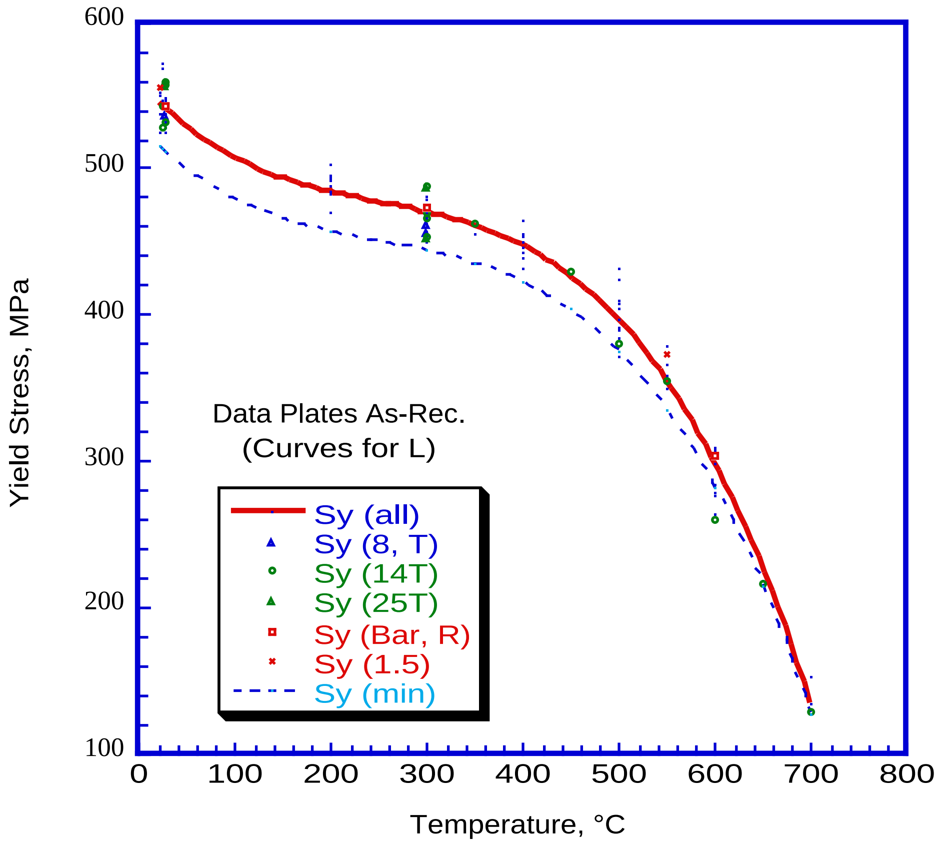

Figure A3.S18E.3.1.2. Yield stress (S_y) of Eurofer base metal plates in transversal orientation and bars in radial direction are bound by minimum curve of L data (CEA, CIEMAT, FZK, NRG data).

Table 3.1.1 presents S_y average and minimum values at temperatures 20 °C through 700 °C.

°C	20	100	200	250	300	350	400	450	500	550	600	650	700
$S_{y,av}$ (MPa) Plate, Bar	546	507	484	477	470	461	447	426	396	354	298	226	135
$S_{y,\,min}$ (MPa) Plate, Bar	516	480	457	451	444	436	423	403	375	335	282	214	128

Table A3.S18E.3.1.1. Average and minimum yield stress values

b. Irradiated conditions

Eurofer irradiation program is still in progress. Some results are already available. Amongst these are those obtained after 0.32 dpa at 300 °C. They show a significant increase in yield and slight increase in ultimate tensile strengths. The reported data also cover low temperature tests (particularly useful for fracture toughness analysis).

Other data are reported following 2.5 dpa irradiation at 60 °C (NRG data). These results show that Sy and Su become almost one. At room temperature the values range from 820 to 880 MPa, while at 300 °C they are about 620 MPa. At temperatures 500 °C and above irradiation hardening tends to disappear.

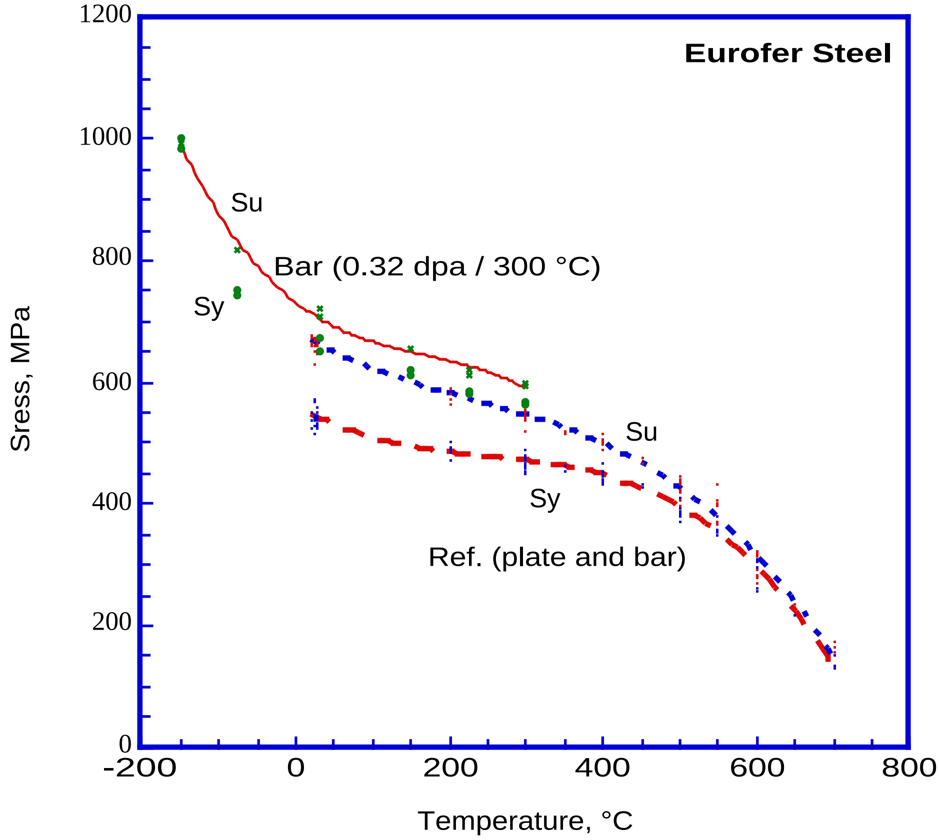

Figure A3.S18E.3.1.3. Effect of irradiation on tensile properties of Eurofer steel (irr. Data from SCK).

A3.S18E.3.2 Minimum and Average Ultimate Tensile Strength: S_u

a. Unirradiated condition

Ultimate tensile strength values obtained from tension tests performed on specimens cut in the longitudinal and transversal orientations of the 8, 14, and 25 mm plates and longitudinal and radial directions of 100 mm bars are shown in Figure 3..2.1.

- Formulae 3.2.1-3.2.2

A 3rd degree polynomial equation is fitted to the experimental data disregarding the specimen orientation.

The scatter of UTS results at room temperature is less than that at 500 °C, therefore, a reduction factor based on 500 °C results is applied ($S_{u\ av}$ = 427 MPa, SD= 15.7 MPa).

$$S_{u\ (av)} = 682.3 - 0.7577\ \theta + 1.7568\ \text{x}10^{-3}\ \theta^2 - 2.5197\ \text{x}10^{-6}\ \theta^3$$

$$S_{u\ (min)} = 0.928*(682.3 - 0.7577\ \theta + 1.7568\ \text{x}10^{-3}\ \theta^2 - 2.5197\ \text{x}10^{-6}\ \theta^3)$$

Equations are valid in the range of 20 °C < θ < 700 °C.

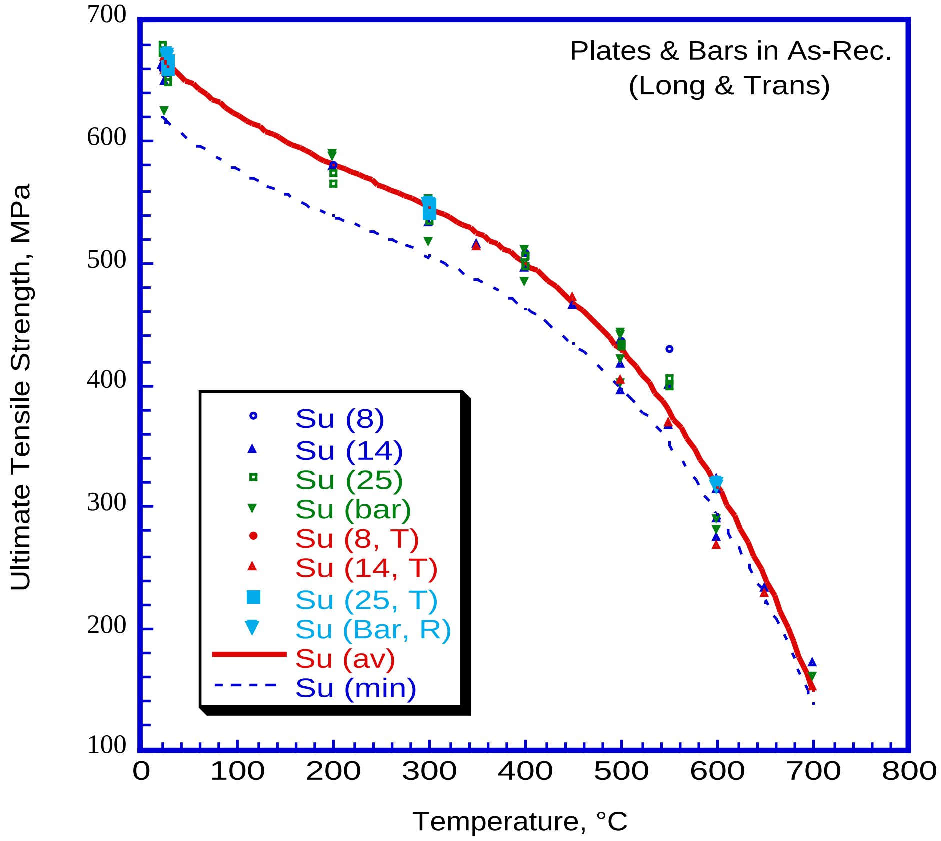

Figure A3.S18E.3.2.1. Ultimate Tensile Strength (S_y) of Eurofer base metal in both orientations versus test temperature (CEA, CIEMAT, FZK, NRG data).

- Table 3.2.1

Table 3.2.1 presents S_u min values at temperatures 20 C through 700 C.

°C	20	100	200	250	300	350	400	450	500	550	600	650	700
$S_{u,\ av}$ (MPa) Plate, Bar	668	622	581	563	545	524	499	467	428	378	316	240	148
$S_{u,\ min}$ (MPa) Plate, Bar	620	577	539	523	506	487	463	434	397	351	293	223	138

Table A3.S18E.3.2.1. Average and minimum ultimate tensile strength values

Tensile properties of powder HIP products are slightly below the minimum curves at room temperature but close to the minimum curves at higher temperatures, Figure A3.S183.3.2.2. In contrast solid HIP properties are well above the average values.

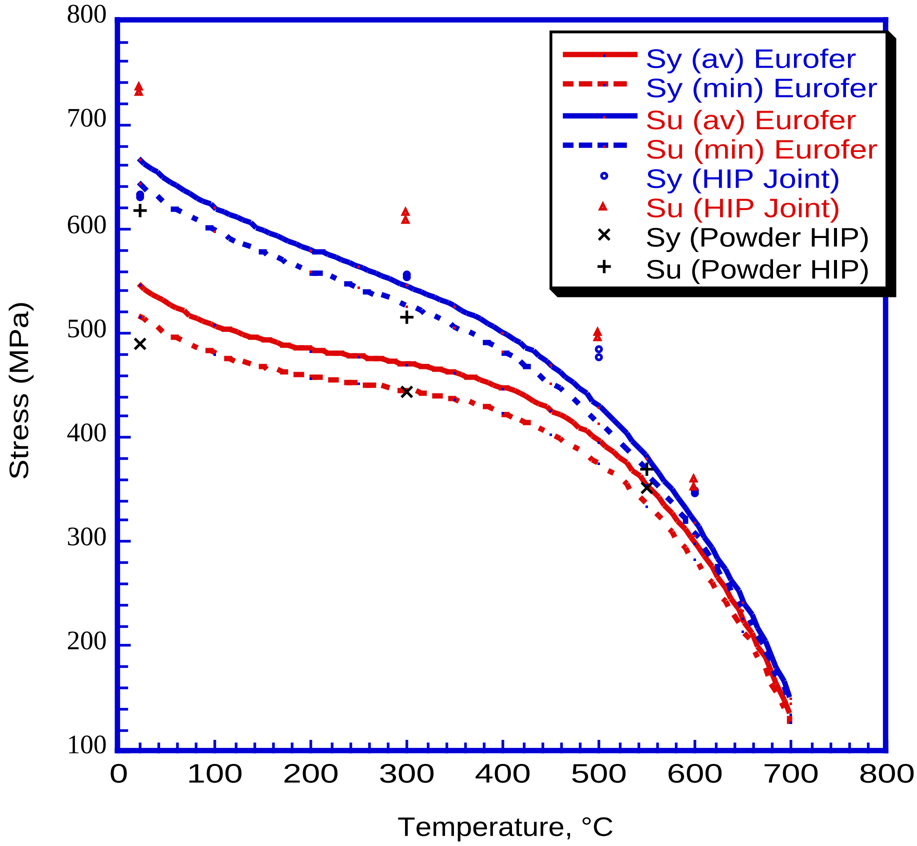

Figure A3.S18E.3.2.2. Powder HIP products have slightly lower resistance than wrought products. In contrast solid HIP joints have a higher resistance (CEA data).

b. Irradiated condition

See section 3.1.1b.

A3.S18E.3.3 Minimum Uniform and Total Elongations: ε_u, ε_t

a. Unirradiated condition

Variations of the uniform tensile elongation versus temperature are shown in figure 3.3.1 for base metal in N&T condition. Solid HIP products show a similar behaviour, with values of about 5% in both bulk and joint areas, but reducing to 0.8% at 600 °C in the joint.

The minimum elongation is observed at 600 °C: ε_u = 0.5%

Variations of the total tensile elongation versus temperature are shown in figure 3.3.2 for base metal in N&T conditions. Solid HIP products show a similar behaviour, with values of about 17 % in both bulk and joint areas, but reducing to 13 % at 300 °C in the joint.

The minimum elongation is observed at 350 °C: ε_t = 13 %

b. Irradiated condition

To be added.

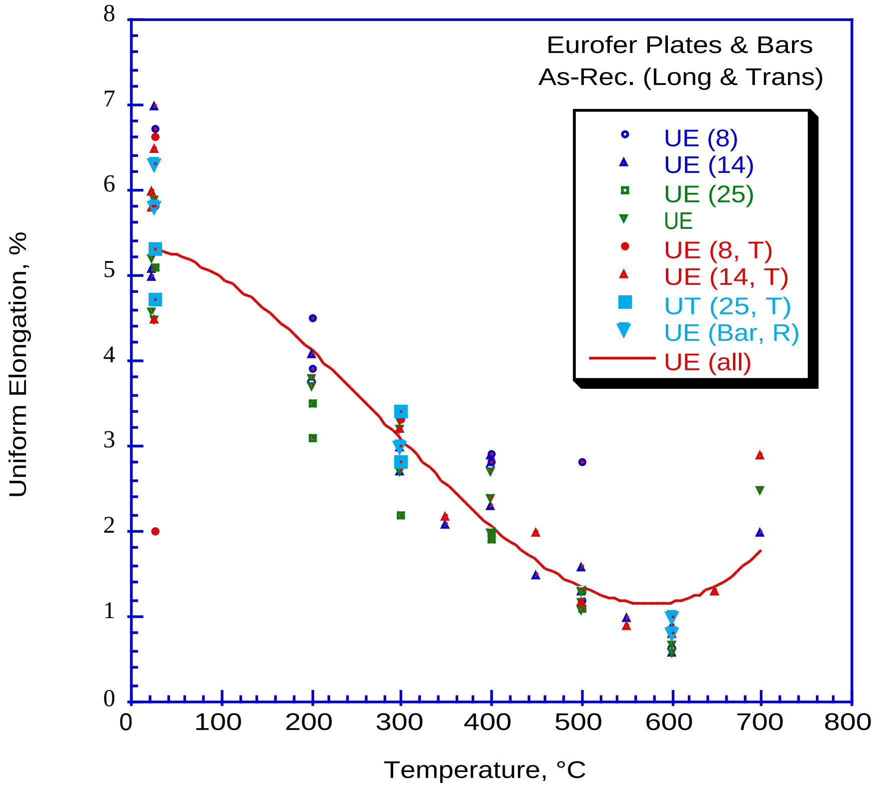

Figure A3.S18E.3.3.1. Uniform tensile elongation of Eurofer base metal versus test temperature (CEA, CIEMAT, FZK, NRG data).

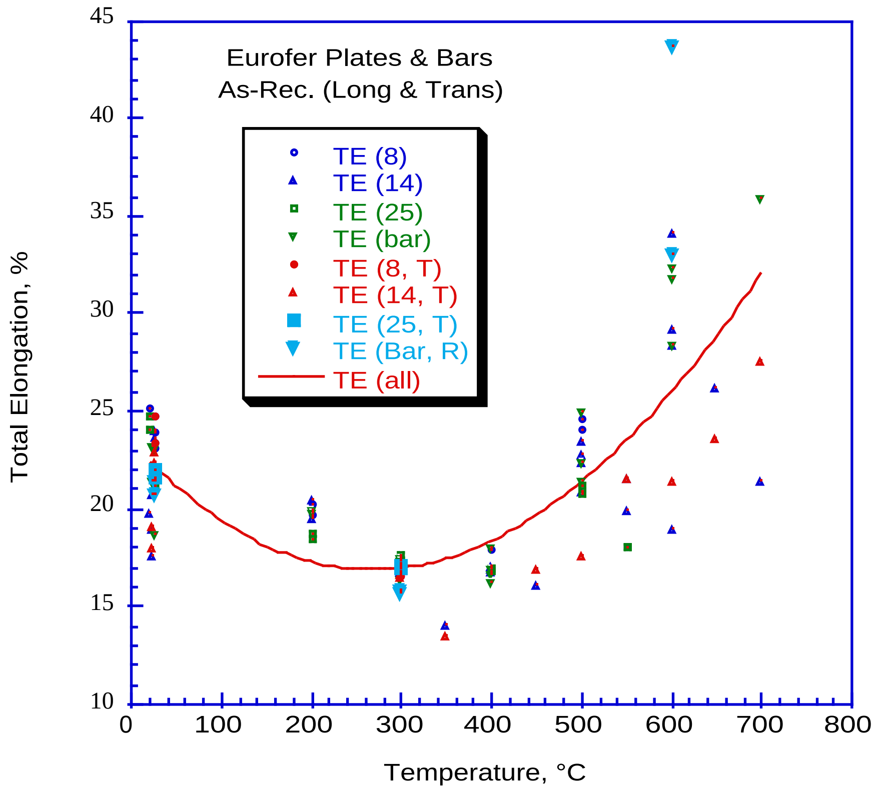

Figure A3.S18E.3.3.2. Total tensile elongation of Eurofer base metal versus test temperature (CEA, CIEMAT, FZK, NRG data).

A3.S18E.3.4 Minimum True Strain at Rupture: ε_{tr}

a. Unirradiated condition

Eurofer steel shows high values of reduction of area, greater than about 70 %. Solid HIP products also show high values.

The minimum true strain at rupture is obtained from equation 3.4.1.

- Formula 3.4.1

$$\varepsilon_{tr} = \ln\left(\frac{100}{100 - \%RA}\right)$$

% RA : reduction in area

ε_{tr} = 1.0

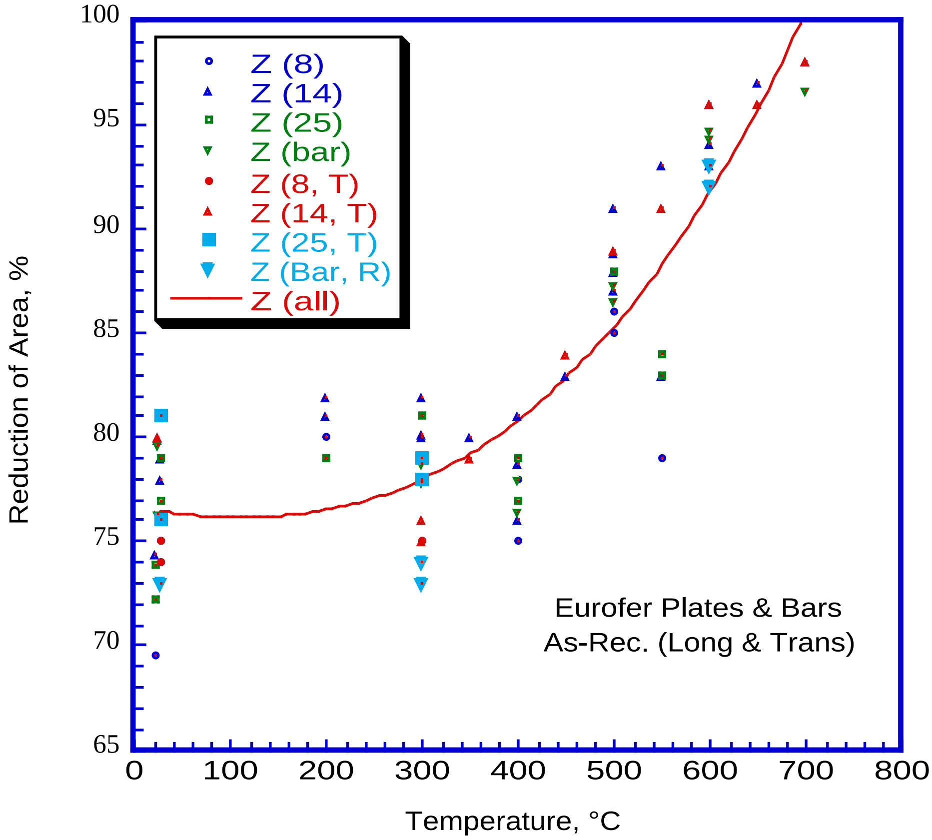

Figure A3.S18E.3.4.1. Reduction of area of Eurofer base metal versus temperature measured after tension test (CEA, CIEMAT, FZK, NRG data).

b. Irradiated condition

To be added.

A3.S18E.3.5 Minimum Time to Creep Rupture: t_r

Creep rupture data of Eurofer steel (in L and T orientations) are collected and plotted versus the Larson-Miller parameter (P). A constant value of 30 is used in P, figure A3.S18E.3.5.1 The effect of test environment on creep rupture life is ignored as most high temperature tests (> 600 °C) are performed in vacuum only.

Average and minimum equations describing creep stress versus P are given by formulae 3.5.1 and 3.5.2 and creep rupture time versus stress by equation, 3.5.3. A good correlation between calculated and experimental values is obtained, figure A3.S18E.3.5.2.

- Formulae 3.5.1 and 2

$$\sigma_{av} = 1950.1 - 88.452\ P + 0.888324\ P^2$$

$$\sigma_{min} = 1950.1 - 88.452\ P + 0.888324\ P^2 - 1.96*7.209$$

- Formulae 3.5.3

$t_r = 10\text{^}((1000/(\theta+273))\ (32.617 - 0.029856\ \sigma + 1.2561\text{x}10^{-5}\ \sigma^2) - 30)$

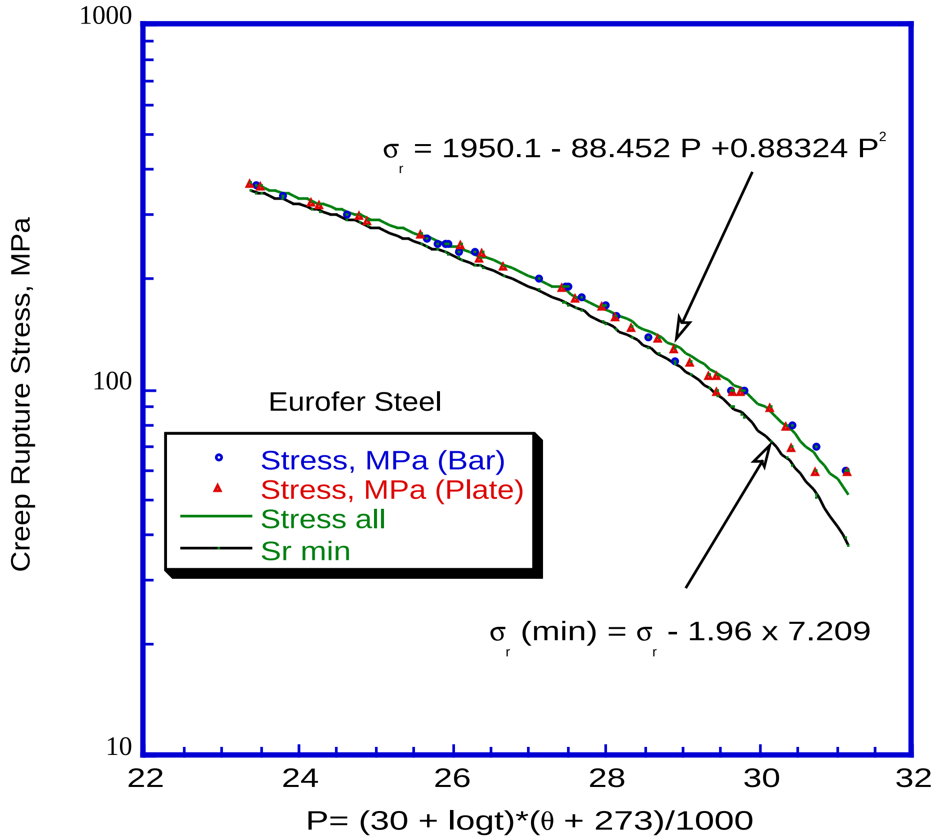

Figure A3.S18F.3.5.1 Creep rupture curve of Eurofer steel (FZK, CIEMAT data).

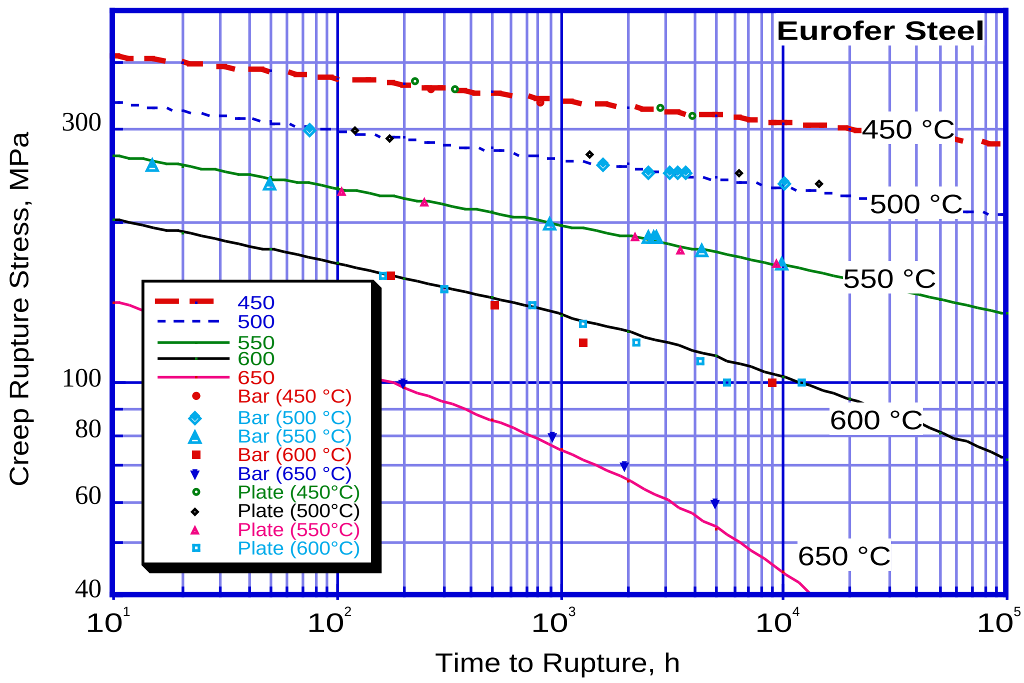

Figure A3.S18E.3.5.2 Comparison of experimental creep rupture results with trends derived from master curve using equation 3.5.1. (Plates data at 650 °C not shown).

A3.S18E.3.6 Minimum Creep Ductility: ε_c

Experimental elongation values at failure recorded for test temperatures 450 °C through 650 °C are plotted in figure 3.6.1. Minimum observed elongation is greater than 15%.

As an interim recommendation, minimum creep ductility is taken ε_c = 15 %.

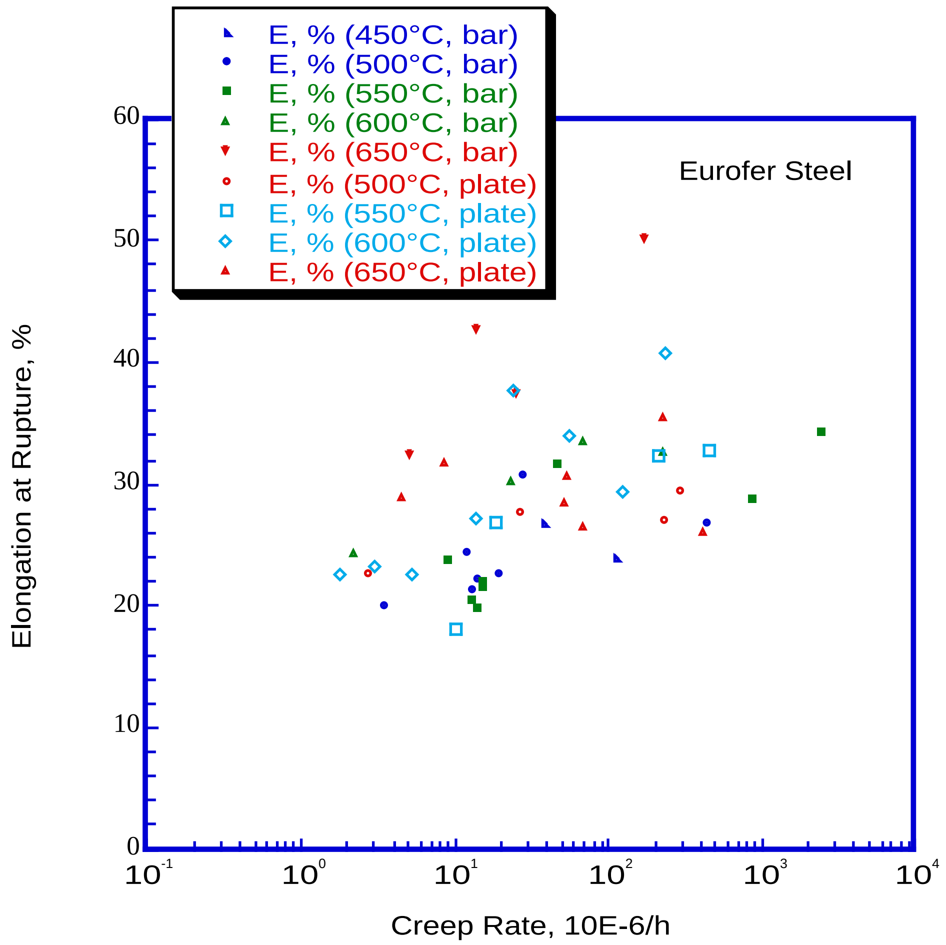

Figure A3.S18E.3.6.1. Experimental data used to derive minimum creep ductility (FZK, CIEMAT data).

A3.S18E.3.7 Minimum True Strain at Rupture for Creep: ε_{ctr}

Experimental values of reduction of area at failure at test temperatures 450 °C through 700 °C are plotted in figure 3.7.1. All recorded values are greater than 60%. However, some laboratories have not reported ROA values in their test results.

Interim value to use:

$$\varepsilon_{ctr} = 1$$

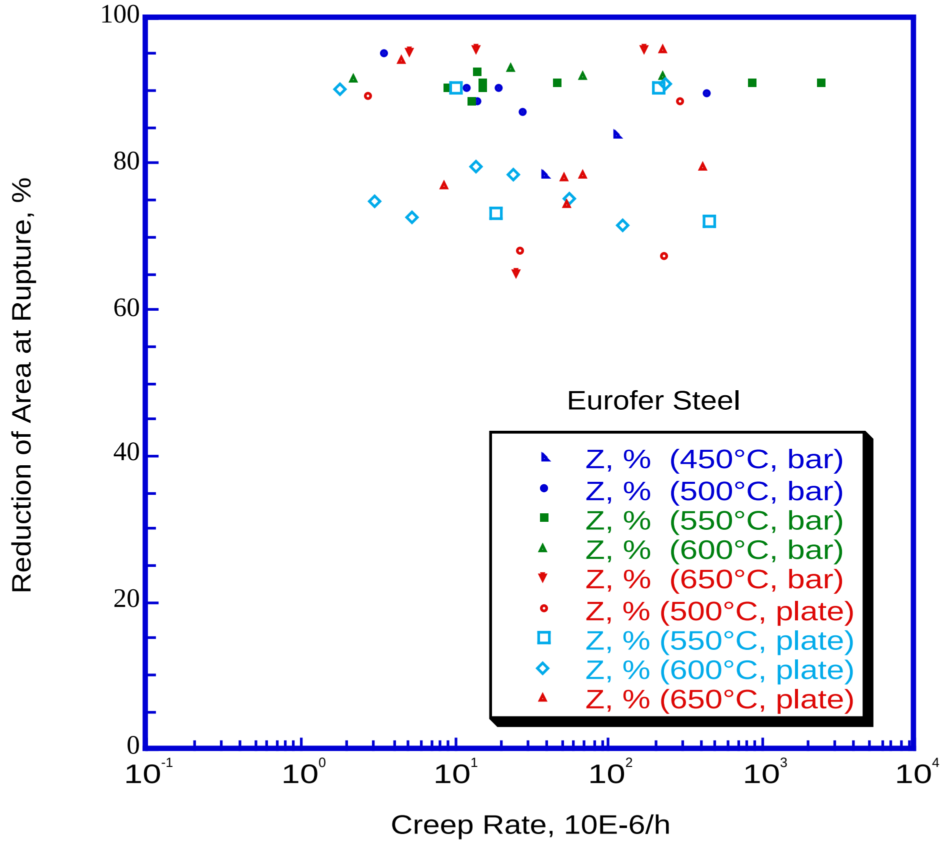

Figure A3.S18E.3.7.1. Experimental data used to derive true creep strain at rupture (FZK, CIEMAT data).

A3.S18E.4 CURVES FOR TESTS ON CREEP AND SWELLING

A3.S18E.4.1 Negligible Thermal Creep Curve

Thermal creep is ignored at temperatures less than 425 °C. At higher temperatures, it is ignored if creep deformation under a stress of 1.5 S_m is less than 0.05 %. Table 4.1.1 shows the values derived from limited data available. Time to reach 0.05% deformation at temperatures 500 °C and above is very short.

- Table 4.1.1

T	1.5 Sm	h
450	217	
500	198	3
550	175	1
600	147	

Table A3.S18E.4.1.1. Negligible thermal creep time limits (t_c)

A3.S18E.4.2 Swelling Curve (ϕt_{s1}) for the Test to Determine if Nonlinear Analysis is Needed

To be added. However, ferritic steels are known for their resistance to swelling.

A.S18F.4.3 Negligible Swelling Curve

To be added

A3.S18E.4.4 Irradiation Induced Creep

To be added

A3.S18E.4.5 Irradiation Induced Creep Curve (ϕt_{c1}) for the Test to Determine if Nonlinear Analysis is Needed

The fluence (ϕt_{c1}) for the test to determine if nonlinear analysis is needed is defined by the fluence to accumulate a creep strain of 2% at a stress of S_m (T,ϕt).

To be added

A3.S18E.4.6 Negligible Irradiation-induced creep curve

The fluence (ϕt_{c2}) for negligible irradiation-induced creep is defined by the fluence to accumulate a creep strain of 0.05% at a stress of 1.5 S_m (T,ϕt).

To be added

A3.S18E.5 ANALYSIS DATA

A3.S18E.5.1 Values of S_m

a. Unirradiated condition

Figure 5.1.1 shows that S_m is governed by S_u values (1/3 of S_u is lower than 0.9 times S_y). It also shows that limited data available on HIPed materials are covered by min curve.

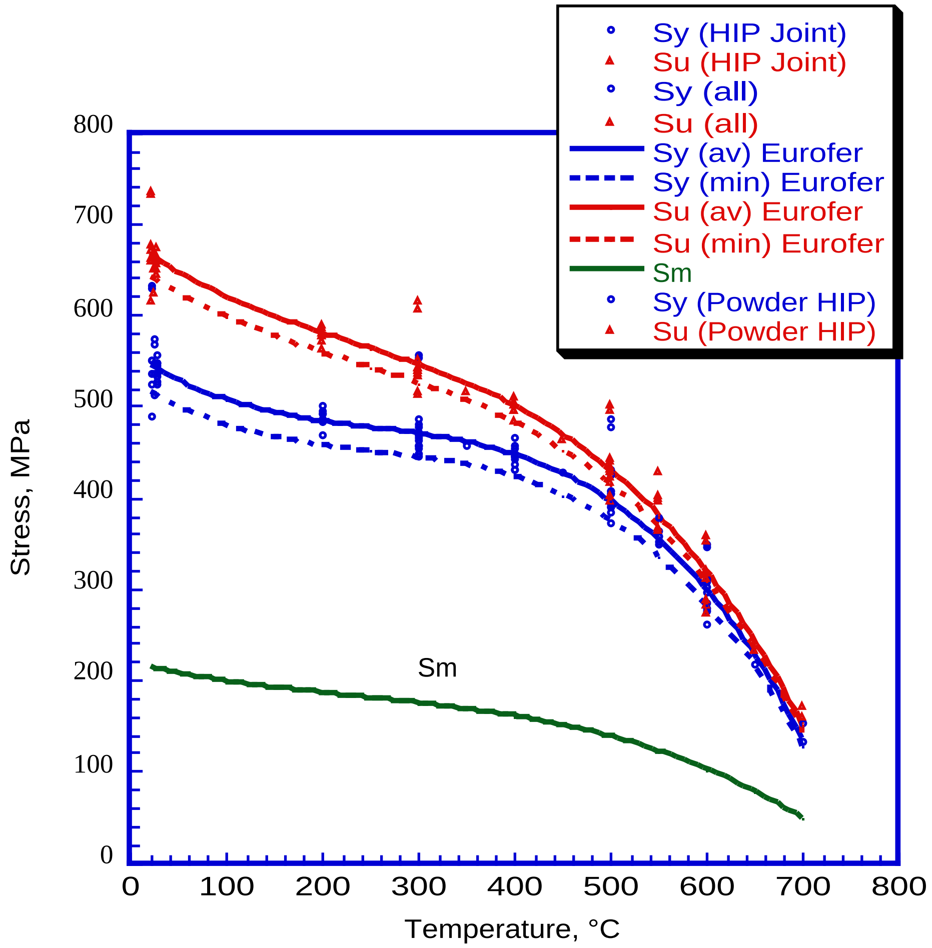

Figure A3.S18E.5.1.1. S_m versus temperature.

- Formula 5.1.1

$$S_m = (666.44 - 0.84514\,\theta + 2.1019{*}10^{-3}\,\theta^2 - 2.617\times10^{-6}\,\theta^3)/3$$

Table 5.1.1

Temp. °C	20	100	200	250	300	350	400	450	500	550	600	650	700
S_m (MPa)	207	192	180	174	169	162	154	145	132	117	98	74	46

Table A3.S18E.5.1.1. S_m at temperatures 20 °C through 700°C.

Effect of ageing has been investigated at several temperatures. At temperatures up to 500 °C, results up to 5000 h of aging show little effect on tensile properties. Results from higher temperature agings show an effect, but the temperatures used are often much higher than the anticipated service temperature for RAFM steels, figure 5.1.2.

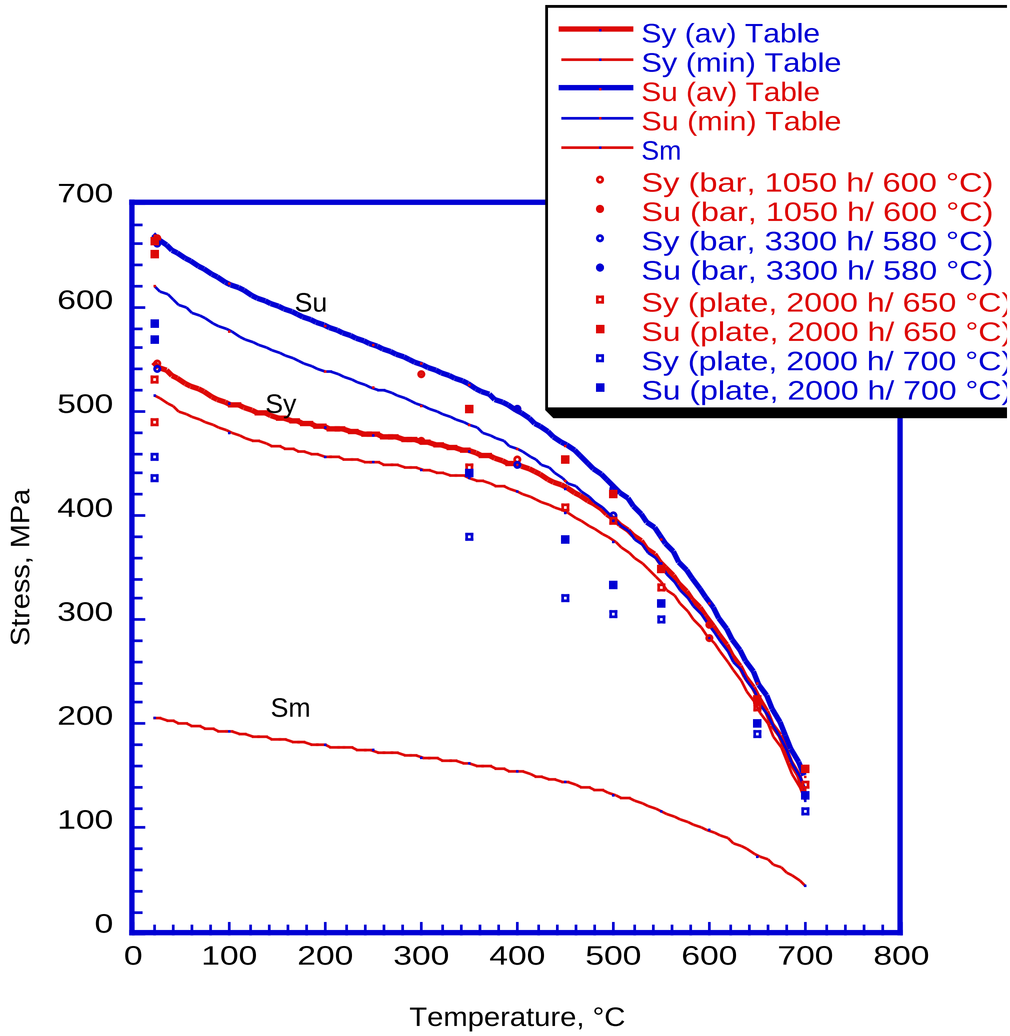

Figure A3.S18E.5.1.2. Effect of aging on tensile properties (CEA, FZK data).

b. Irradiated condition

Unirradiated values will govern design.

A3.S18E.5.2 Values of S_t

a. Unirradiated condition

Maximum allowable values of stress S_t at a given temperature for a given time are derived from 2/3 of minimum stress to rupture and are reported in table 5.21 (stress values are in MPa, temperatures in °C and times in hours).

Notice that St is derived from three criteria: 2/3 S_r (θ, t), 80% of minimum stress to end of secondary creep in time t, and minimum stress isochronous curve that results in 1% deformation (elastic + plastic + creep). Figure 5.2.1 shows the stress for time to reach 1% creep deformation and rupture as a function of LM. Eurofer end of secondary creep data are insufficient and are not used in S_t analysis.

$$S_{1\%\ ave} = 2908.9 - 164.39\ P + 2.331\ P^2$$

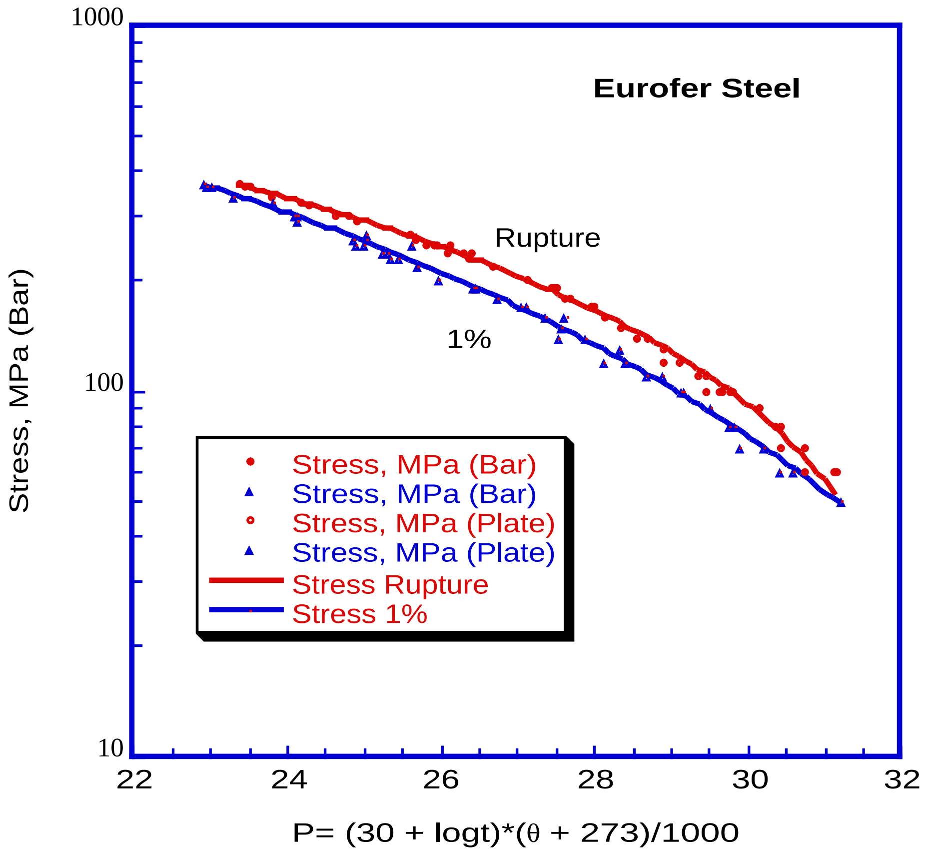

Figure A3.S18E.5.2.1. Comparison of creep rupture stress and stress to 1% creep deformation (FZK, CIEMAT data).

Time (h)	425°C	450°C	475°C	500°C	525°C	550°C	575°C	600°C	625°C	650°C	675°C
10	290	265	240	216	192	169	147	126	105	85	66
30	279	254	229	204	181	158	136	115	94	74	55
100	267	242	217	192	169	146	124	103	82	63	44
300	256	231	206	181	158	135	113	92	72	52	33
1000	245	219	194	170	146	123	102	81	60	41	22
3000	234	208	183	159	136	113	91	70	50	31	12
10000	223	197	172	148	124	102	80	59	39	20	
30000	213	187	162	137	114	92	70	49	29	10	
100000	201	176	150	126	103	81	59	39	19		
300000	191	166	140	116	93	71	50	29	10		

Table A3.S18E.5.2.1. Values of S_t for Temp. 425-675°C

b. Irradiated condition

To be added

A3.S18E.5.3 Creep Rupture Stresses, S_r

a. Unirradiated condition

Minimum stress rupture values, S_r , derived from equation 3.5.2 are given in the table 5.3.1 for several test temperatures and are plotted in figure 5.3.1. Stress values are in MPa, temperature in °C and time in hours.

- Table 5.3.1

Time (h)	425°C	450°C	475°C	500°C	525°C	550°C	575°C	600°C	625°C	650°C	675°C
10	436	397	360	324	288	254	221	189	158	128	99
30	419	380	343	307	271	237	204	172	141	112	83
100	401	362	325	288	253	219	186	154	124	94	66
300	385	346	308	272	237	203	170	138	108	78	50
1000	367	328	291	254	219	185	152	121	90	61	33
3000	351	313	275	238	203	169	137	105	75	46	18
10000	334	295	258	221	186	152	120	89	59	30	
30000	319	280	242	206	171	137	105	74	44	16	
100000	302	263	226	189	155	121	89	58	28		
300000	287	248	211	175	140	106	74	44	14		

Table A3.S18E.5.3.1. Values of S_r at Temperatures 425 to 675°C.

b. Irradiated condition

To be added

A3.S18.5.4 Fatigue Curves at Saturation

To be added

A3.S18E.5.5 Isochronus and Creep Deformation Curves

To be added

b. Irradiated condition

To be added

A3.S18E.5.6 Values of S_{Rh} and S_{Rc}

a. Unirradiated conditions

Not available for RAFM steels. Those of Mod. 9Cr1Mo are used as an interim step.

- Formula 5.6.1

Using a cycle with relaxation form most representative of the average relaxation throughout the fatigue life of Mod 9Cr-1Mo steel, results are fitted with:

$$\sigma = \sigma_{max} / \exp(at^b)$$

Here, σ_{max} is the stress at the start of the relaxation, and σ (MPa) is the relaxed stress at time t (minutes) and, b and a are constants. Values of b are approximately constant and around 0.2, while those of a vary according to σ_{max}.

- Table 5.6.1

To be added

- Figure 5.6.1

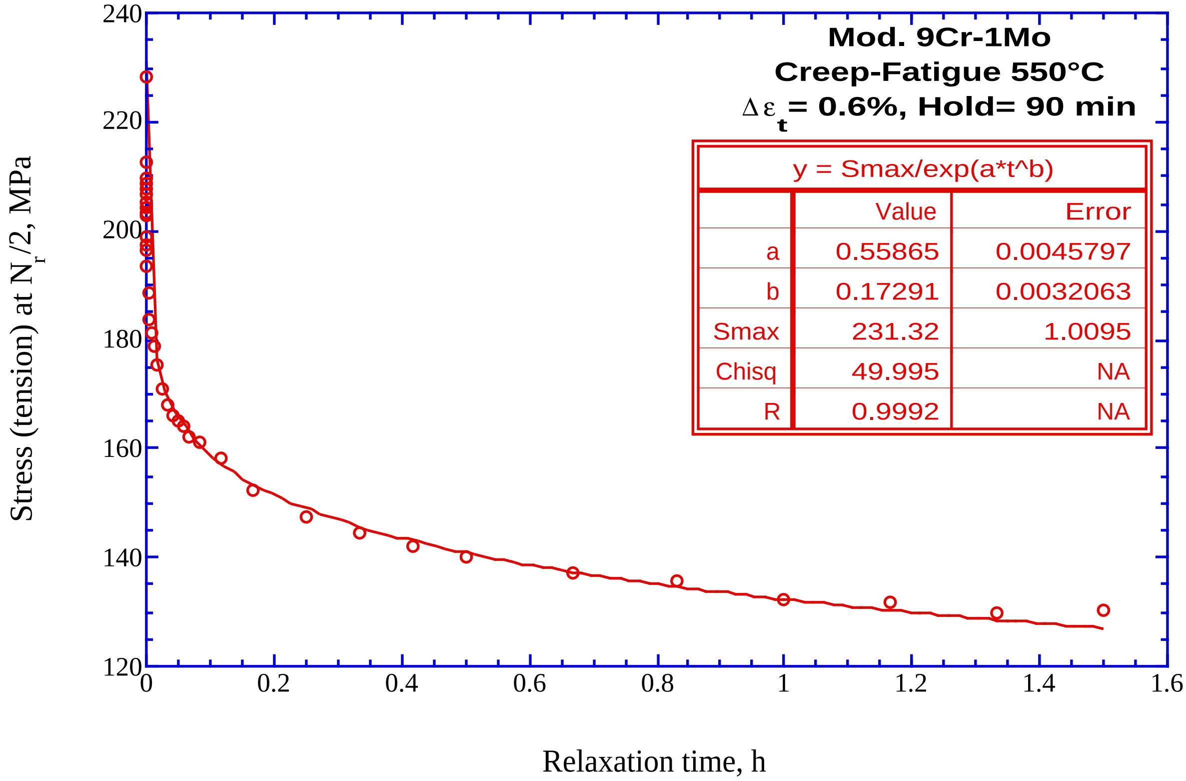

Figure A3.S18E.5.7. Example of a curve fitted to hold time relaxation data of Mod 9Cr-1Mo steel (CEA data)

A3.S18E.5.7 Symetrisation factor, K_S

Not available for RAFM steels.
Also, it has been noted that Mod 9Cr1Mo steel is very sensitive to creep strain effects. This sensitivity together with softening behaviour of the steel does not allow calculation of a symetrisation factor from presently available experimental data.
The available data for Eurofer steel show the tendency towards mean compressive stress towards the end of fatigue life. An example of this evolution is shown in figure A3.S18E.5.8. The test is performed at 450 °C at a total strain range of 1.5%. Lower strain ranges also show a similar trend.

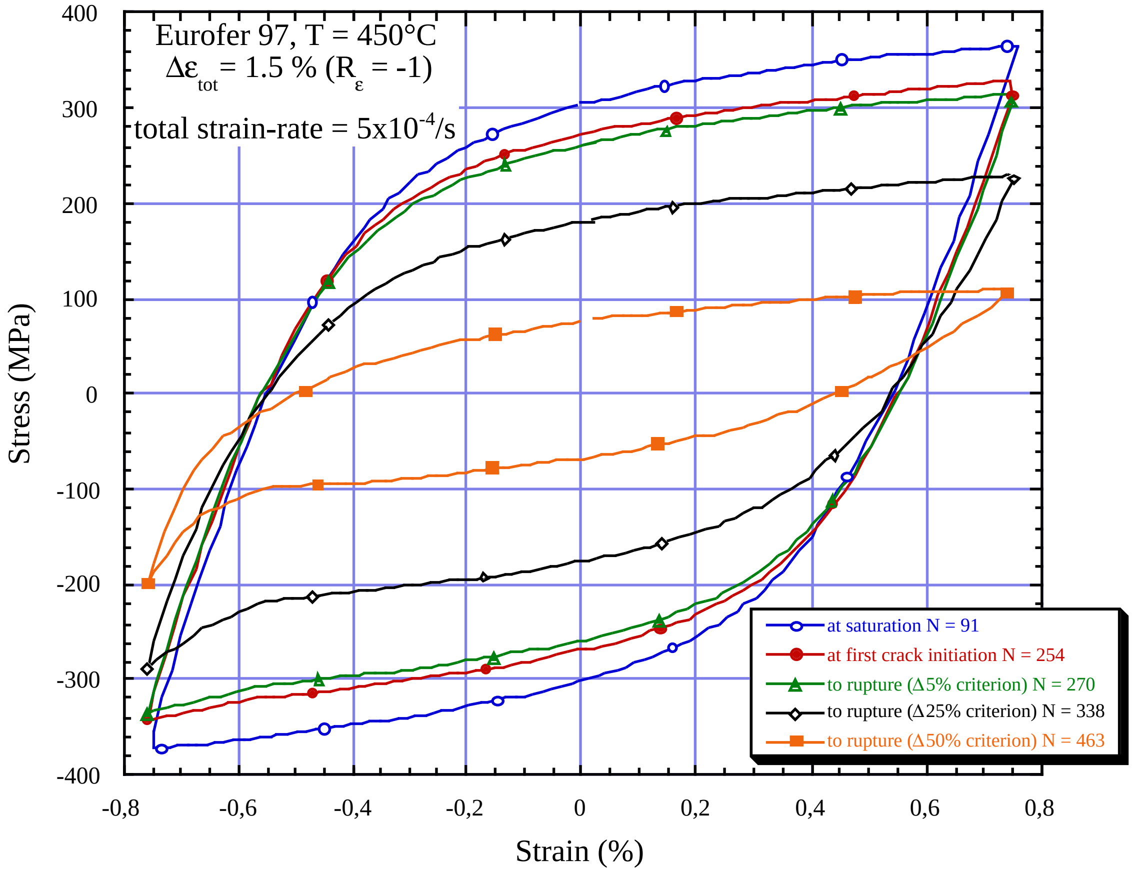

Figure A3.S18E.5.8. Example of the evolution of hysteresis loop during strain controlled fatigue cycling of Eurofer steel. (ENEA data)

A3.S18E.5.8 Creep-Fatigue Interaction Diagram

Insufficient experimental data

A3.S18E.5.9 Cyclic Curves, Values of K_ε and K_ν

A3.S18E.5.9.1 Cyclic Curves

a. Unirradiated condition

Total strain range can be expressed in terms of elastic and plastic strains ranges:

($\varepsilon_t = \varepsilon_e + \varepsilon_p$)

Where $\varepsilon_e = \sigma/E$ and $\varepsilon_p = A\sigma^n$ or $\sigma = K\varepsilon_p{}^m$.

In this paper, the elastic strain component is calculated ($\varepsilon_e = \sigma/E$) and then deducted from the total strain to obtain the plastic strain component (reported data often do not include plastic strain). S_{ao} is the maximum stress in tension at the first cycle (monotonic) and $\Delta\sigma/2$ is half stress range at half-life (cyclic), both are in MPa. Modulus (E) values of F82H steel are used.

Notice that the initial stress at maximum strain may drop sharply during the first few cycles (at high strain ranges) or after an initial hardening (at low strain ranges). The drop becomes milder until about 80% of life, where it becomes sharper again, see Annex 5. The value of stress at Nr/2 is hence an approximate saturation stress value. In creep-fatigue calculation, the drop in stress may reduce creep damage, but as seen from the figures in Annex 5, the drop in stress in the last 20% of fatigue life is too steep to be due to rearrangement of the dislocation structure.

- Table 5.9.1.1 Coefficients)

	450 °C		500 °C		550	
	Mono	Cyclic	Mono	Cyclic	Mono	Cyclic
K	545.17	355.4	493	323.8	450.4	277.32
m	0.14467	0.0457	0.1415	0.0772	0.11787	0.0661

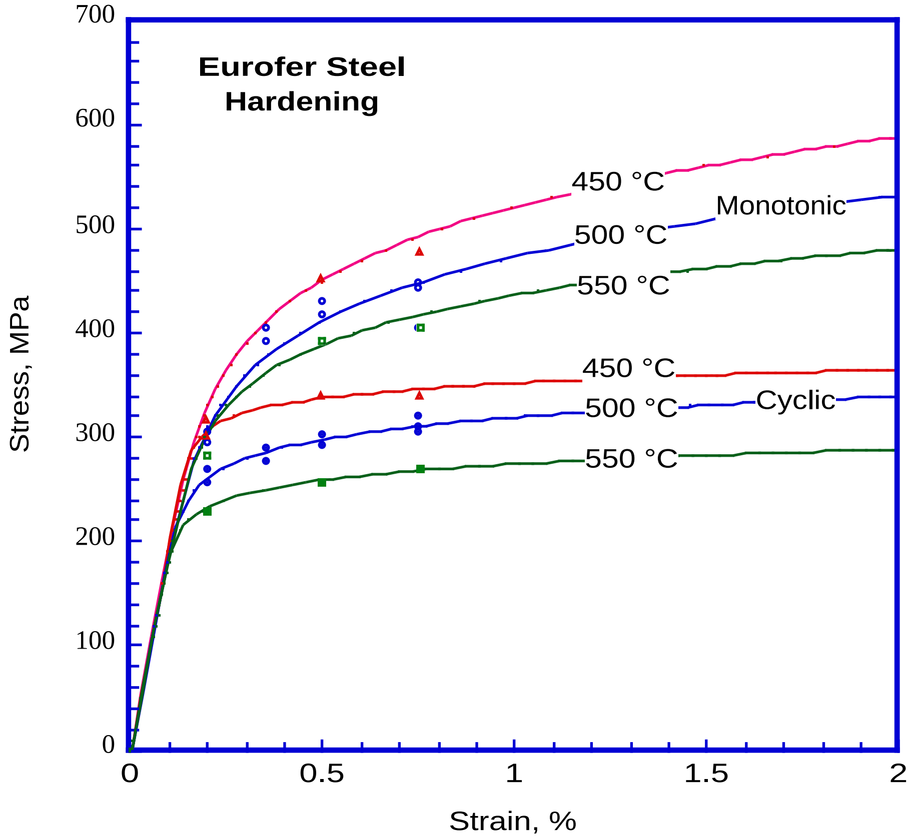

Figure A3.S18E.5.9.1.1. Comparison of monotonic and cyclic hardening curves using dynamic modulus (CIEMAT & ENEA data).

b. Irradiated condition

To be added

A3.S18E.5.92 Coefficient, K_ε

Values of K_ε are deducted from

$$\overline{\Delta\varepsilon_1} = \frac{2(1+\nu)}{3E}\overline{\Delta\sigma_{tot}}$$

$$\overline{\Delta\sigma_{tot}}\,\overline{\Delta\varepsilon_1} = \overline{\Delta\sigma}\,(\overline{\Delta\varepsilon_1} + \overline{\Delta\varepsilon_3})$$

$$\overline{\Delta\varepsilon_1} + \overline{\Delta\varepsilon_3} = \frac{2(1+\nu)}{3E}\overline{\Delta\sigma} + 0.01(\frac{\overline{\Delta\sigma}}{K})^{1/m}$$

$$K_\varepsilon = \frac{\overline{\Delta\varepsilon_1} + \overline{\Delta\varepsilon_3}}{\overline{\Delta\varepsilon_1}}(\overline{\Delta\varepsilon_2} negligible)$$

A3.S18E.5.93 Coefficient, K_ν

To be added

- ***Table 5.9.1.2. Monotonic and Cyclic hardening values***

Stress	ε_t % (450 °C)		ε_t % (500 °C)		ε_t % (550 °C)	
MPa	Monotonic	Cyclic	Monotonic	Cyclic	Monotonic	Cyclic
0	0	0	0	0	0	0
10	0.0052	0.0052	0.0053	0.0053	0.0054	0.0054
20	0.0103	0.0103	0.0106	0.0106	0.0109	0.0109
50	0.0258	0.0258	0.0265	0.0265	0.0272	0.0272
100	0.0516	0.0515	0.0529	0.0529	0.0544	0.0543
120	0.0619	0.0619	0.0635	0.0635	0.0652	0.0652
140	0.0722	0.0722	0.0742	0.0741	0.0761	0.0761
160	0.0827	0.0825	0.0850	0.0848	0.0871	0.0872
180	0.0933	0.0928	0.0960	0.0957	0.0982	0.0993
200	0.1041	0.1031	0.1075	0.1078	0.1097	0.1158
220	0.1153	0.1134	0.1197	0.1231	0.1219	0.1496
240	0.1272	0.1239	0.1332	0.1476	0.1352	0.2426
260	0.1400	0.1351	0.1484	0.1958	0.1508	0.5180
280	0.1543	0.1498	0.1665	0.3003	0.1699	1.3082
300	0.1707	0.1793	0.1886	0.5307	0.1949	3.4469
320	0.1901	0.2661	0.2165	1.0275	0.2290	
340	0.2135	0.5553	0.2523	2.0620	0.2768	
360	0.2423	1.5098	0.2989		0.3451	
380	0.2784		0.3599		0.4430	
400	0.3238		0.4399		0.5828	
420	0.3813		0.5444		0.7810	
440	0.4541		0.6804		1.0594	
460	0.5462		0.8562		1.4459	
480	0.6622		1.0819		1.9768	
500	0.8077		1.3693		2.6978	
520	0.9893		1.7328			
540	1.2146		2.1889			
560	1.4925		2.7572			
580	1.8333					
600	2.2488					

A3.S18E.6 ADDITIONAL ANALYSES

A3.S18E.6.1 Monotonic hardening curve in tension

Full curve plots are shown in figures 6.1.1., 6.1.2 and 6.1.3. If the apparent modulus is used for work hardening curves, a good fit is obtained, figures 6.1.4.

Work hardening parameters derived from tension tests are different from those calculated using the dynamic modulus of elasticity (see cyclic hardening curve section). Using 500 °C plot of figure 6.1.2, the work hardening equation:

$\varepsilon\% = 100 * \sigma/E + (\sigma/k)\ 1/m$

where E= 34300 MPa, k= 437.05 MPa, m= 0.06715.

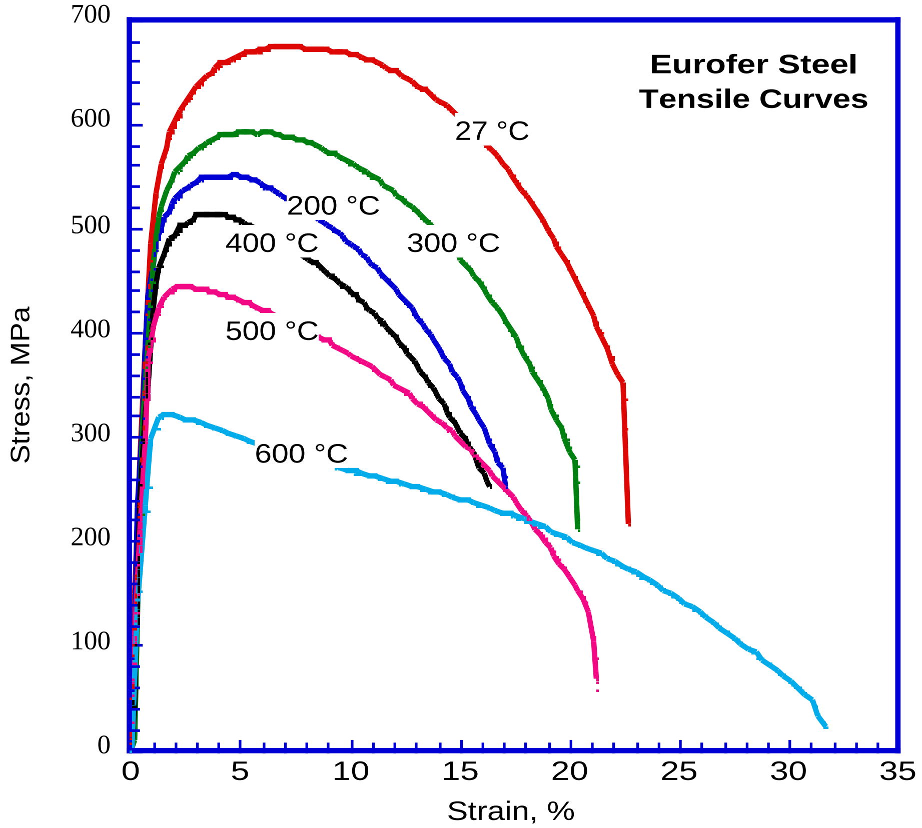

Figure A3. S18E.6.1.1. Tension curves obtained from tests on specimens taken in longitudinal direction of bar 100 mm product (NRG data).

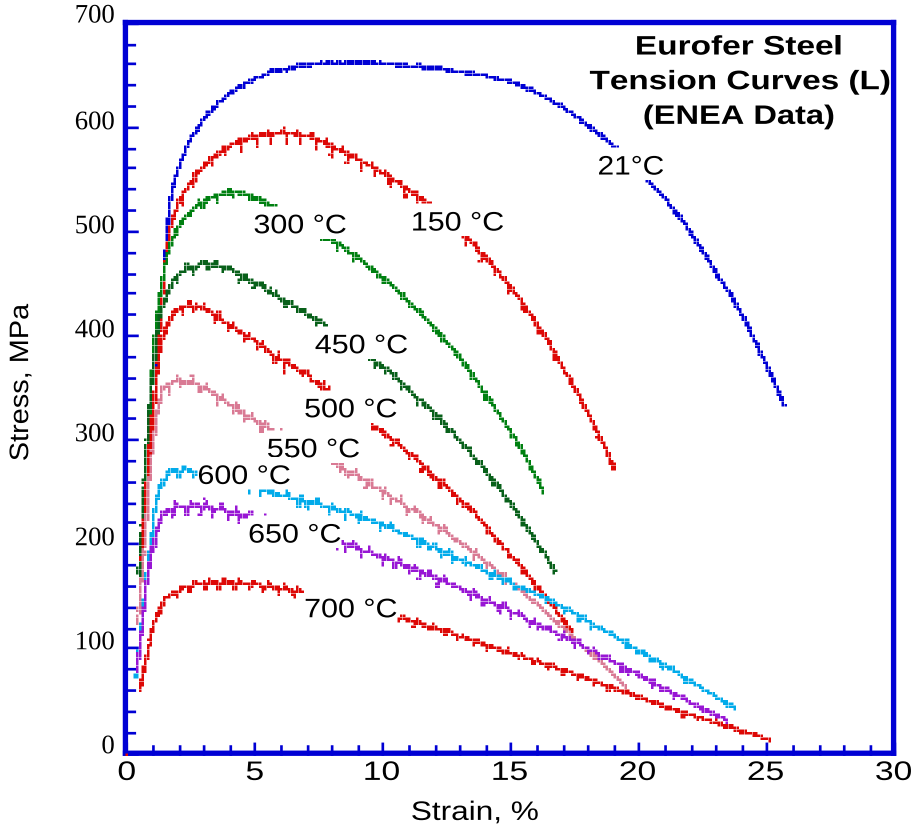

Figure A3. S18E.6.1.2. Tension curves obtained from tests on specimens taken in longitudinal direction of 25 mm plate (ENEA data).

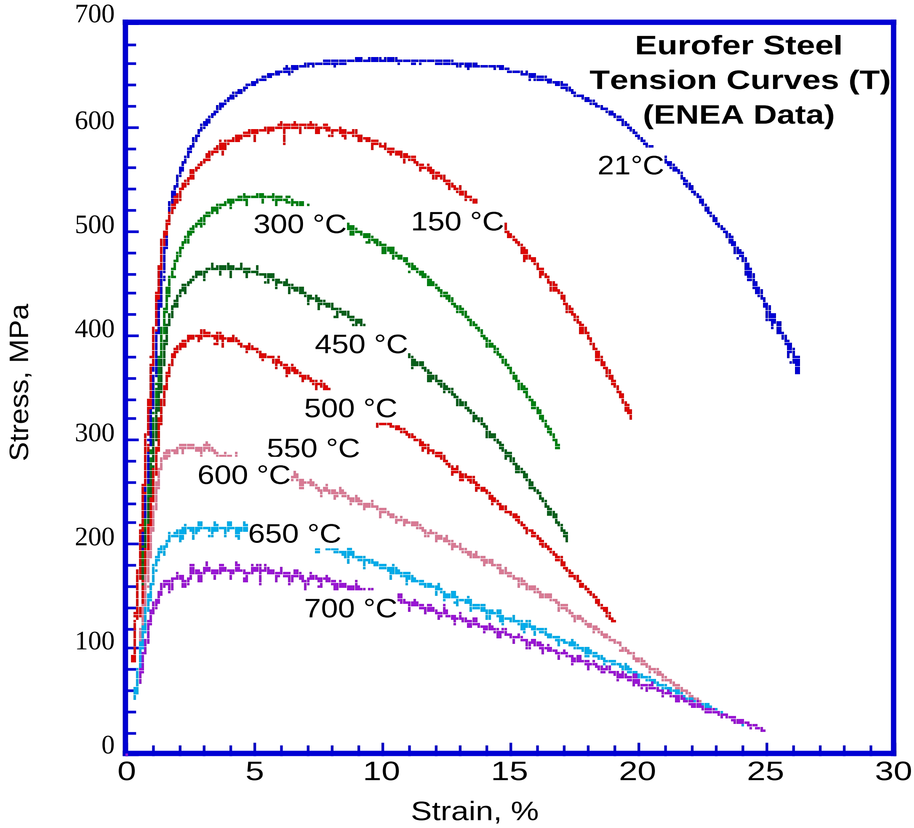

Figure A3. S18E.6.1.3. Tension curves obtained from tests on specimens taken in transversal direction of 8 mm plate (ENEA data).

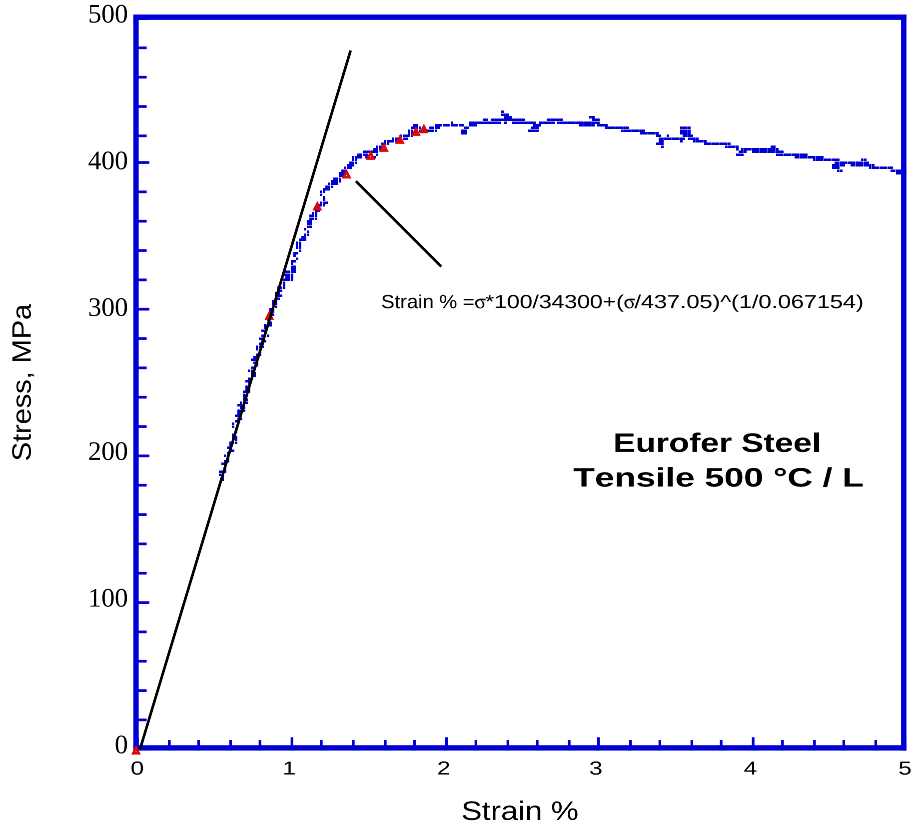

Figure A3. S18E.6.1.4. Work hardening curve obtained using apparent modulus of elasticity, Eurofer plate, 25 mm thickness (ENEA data).

A3.S18E.6.2 Bilinear curves

To be added

A3.S18E.6.3 Creep Deformation Curve

A3.S18.6F.3.1 Primary Creep

a. Unirradiated condition

To be added

A3.S18E.6.3.2 Secondary Creep

At temperatures less than 425 °C secondary creep is ignored.

- equation 6.3.2.1

Secondary creep rate is expressed by:

$$\varepsilon'_S = C\,\sigma^n$$

Where ε'_S is in /h an σ in MPa. Coefficient C and exponent n in equation 6.3.2.1 are obtained from plots of stress versus secondary creep rate, figure 6.3.2.1. Notice that there is an apparent change in the slope of curve at 650°C but this change is ignored for values given in table 6.3.2.1.

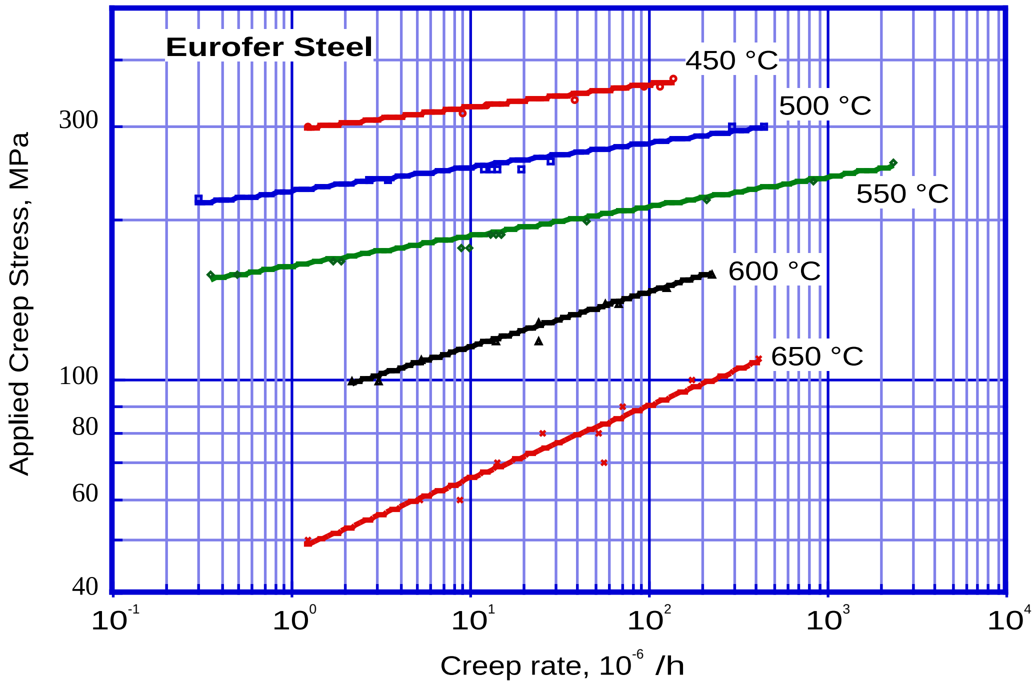

Figure A3.S18E.6.3.2.1. Stress versus minimum creep rate (CIEMAT, FZK data).

- Table 6.3.2.1

ε in %, θ in °C, ε' in 10^{-6} /h, σ in MPa

	$\varepsilon'_s = C\,\sigma^n$	
Temperature, C	C	n
450	8.352×10^{-57}	22.718
500	1.3758×10^{-50}	21.19
550	4.566×10^{-40}	17.769
600	2.4898×10^{-19}	9.5095
650	6.2167×10^{-12}	6.7473
Eurofer		

Table A3.S18E.6.3.2.1. Norton law parameters

When the temperature is equal or greater than 425 °C and the deformation is higher than that at the end of primary creep (ε_{epc}), then secondary creep strain is added to the primary creep strain:

- equation 6.3.2.2

$$\varepsilon_c = \varepsilon_{epc} + 100\, C\sigma^n\,(t - t_{epc})$$

To be added

A3.S18E.6.4 Fatigue Curves

a. Unirradiated condition

Insufficient strain controlled fatigue data are available for reliable analysis. Limited data reported by CIEMAT (500 °C) and ENEA (450 and 550 °C) are used here. Curves are fitted to CIEMAT data. A 50% drop in saturation stress is used to define Nr for ENEA data.

Unlike stainless steels, where a clear saturation stage is observed and the number of cycles to rupture is close to the end of this stage (often a 25% drop in saturation stress is used to calculate Nr), the drop in pseudo saturation stage for FM steels has a slope and can continue for a while before specimen is broken. Detailed microstructural and fractographical examinations are needed to determine the cause of the drop and if necessary use N25 instead of N50 for Nr.

Several thermal fatigue tests have also been performed but the results are not as yet converted to equivalent strain controlled tests (ENEA, FZK).

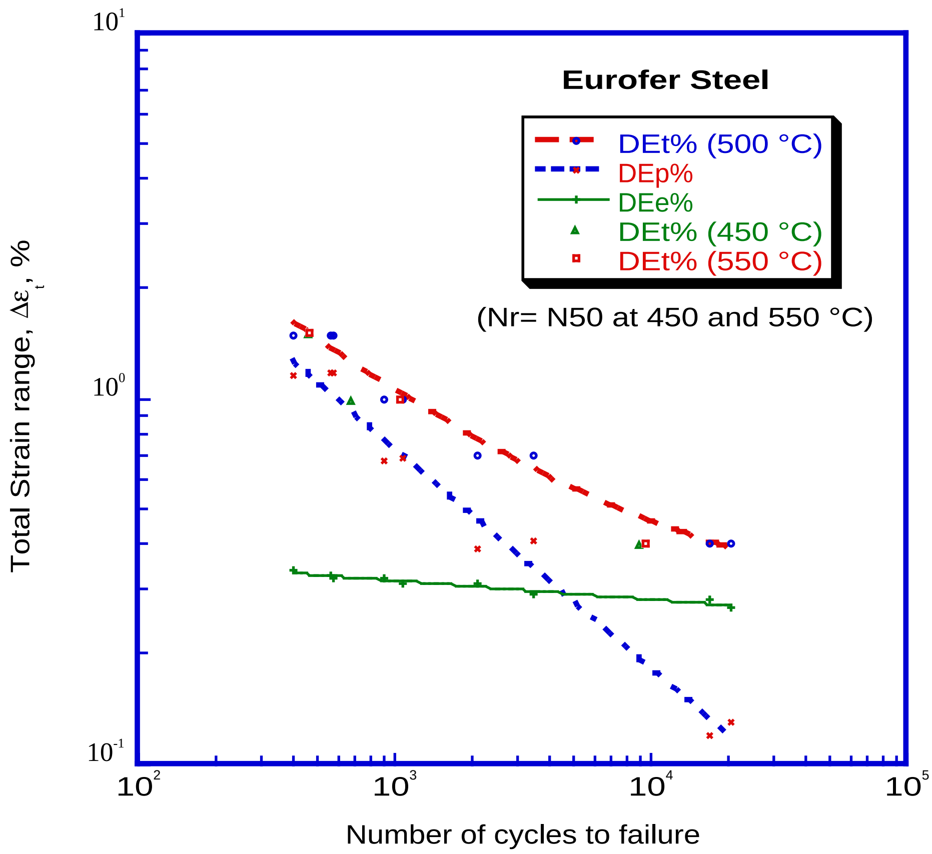

Figure A3.S18E.6.4.1. Low Cycle Fatigue curve of Eurofer steel. Curves fitted to the total strain range (Langer) and elastic and plastic components (Manson-Coffin), (CIEMAT data).

$\varepsilon_t = 0.24483 + 42.876\ N^{-0.575}$
$\varepsilon_p = 46.729\ N^{-0.60272}$, $\varepsilon_e = 0.4521\ N^{-0.05137}$

b. Irradiated condition

To be added

A3.S18E.6.5 Maximum allowable deformation: D_{max}

D_{max} = 1%

A3.S18E.6.6 Toughness

A3.S18E.6.6.1. Impact toughness

a. Unirradiated conditions

Eurofer steel exhibits like other bcc structure metals a transition from ductile mode of fracture to a brittle mode of fracture with decreasing test temperature (DBTT). Figure 6.6.1 shows an example of the data obtained from Charpy impact tests performed on standard 10x10x55 mm V-notch specimens. In this figure the absorbed energy is plotted versus the test temperature. Normalized values in J/cm^2 can be obtained by dividing the J values by 0.8 cm^2.

As it can be seen the 14 mm Eurofer steel plate has a DBTT temperature less than – 50 °C in the normalized and tempered condition (as-received).

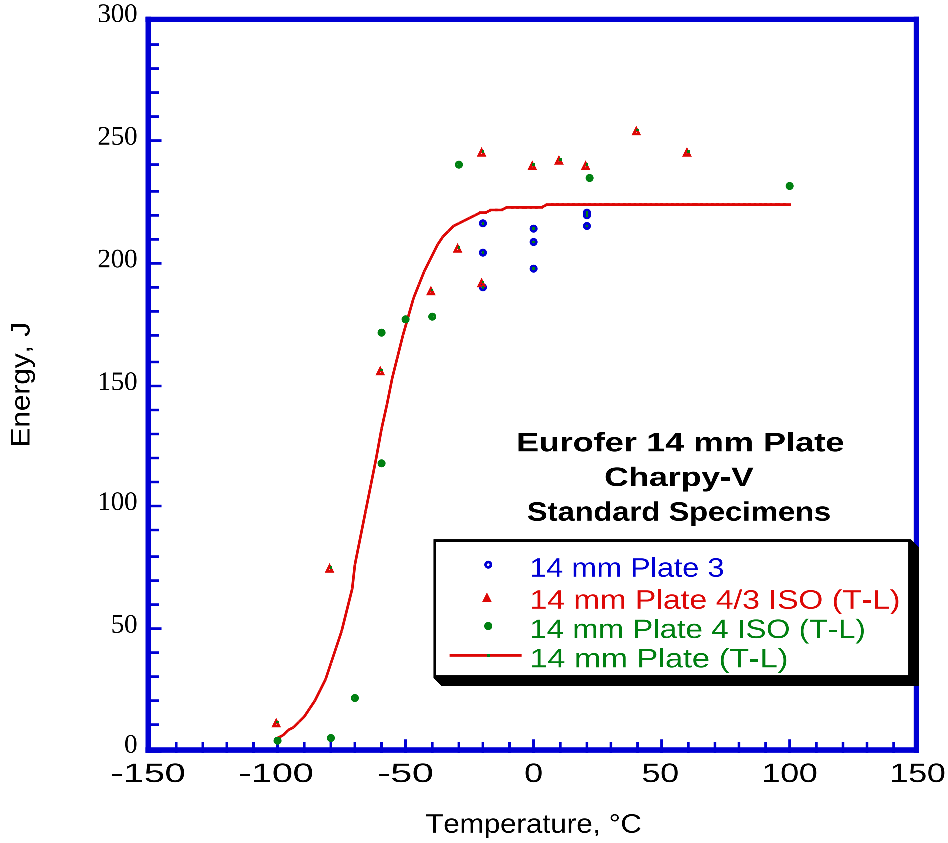

Fig. A3.S18E.6.6.1. Impact toughness of Eurofer base metal in the as-received conditions (Boehler, CEA, FZK data).

- equation 6.6.1

$$J = 111.88 + 111.88\ \exp.((\theta + 63.141)/19.875)$$

Where J is in Joules and θ in °C. The DBTT is –63 °C and the upper shelf energy 222 J (277.5 J/cm^2).

Most of the tests are, however, performed on smaller specimens. Figure 6.6.2 shows the results obtained for KLST (3x4x27 mm) specimens. In general smaller specimens give more optimistic results. The DBTT obtained with the KLST specimens in the present case is around – 100 °C.

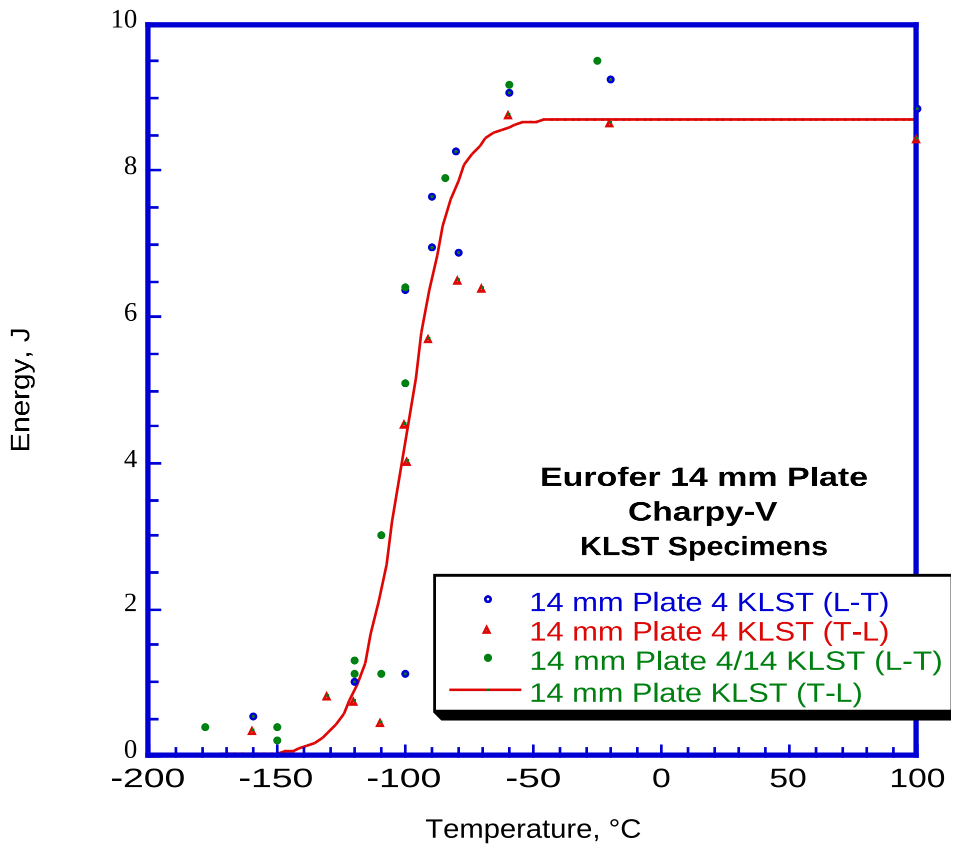

Fig. A3.S18E.6.6.2. Impact toughness of Eurofer base metal in the as-received conditions (KLST specimens), (CEA, NRG data).

- equation 6.6.2

$$J = 4.3594 - 4.3594\ \exp.((\theta + 100.16)/18.299)$$

Where J is in Joules and θ in °C. The DBTT is –100 °C and the upper shelf energy 8.8 J.

The type and size of the products may also affect the results, but as shown in figure 6.6.3, the scatter is small for Eurofer plates (8, 14 and 24 mm thick) and 100 mm diameter bars. The effect of specimen orientation is also negligible.

Diffusion bonded specimens show a behavior similar to the bulk material after HIPing (2h at 1100 °C, 100 MPa, followed by PBHT (1h 750 °C, 1h 950 °C, 1 h 750 °C). The upper shelf energy of HIPed specimens (U notch) compared with reference material (V-notch) is lower, figure 6.6.4.

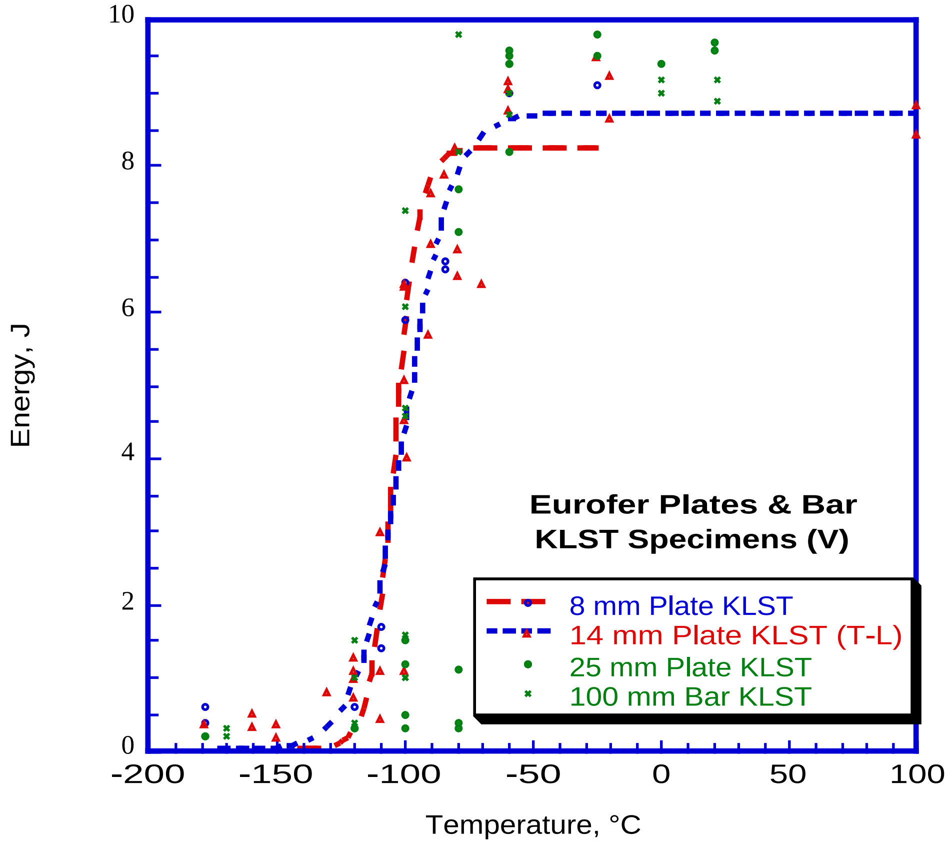

Fig. A3.S18E.6.6.3. Impact toughness of Eurofer base metal in the as-received conditions (KLST specimens), (CEA, NRG data).

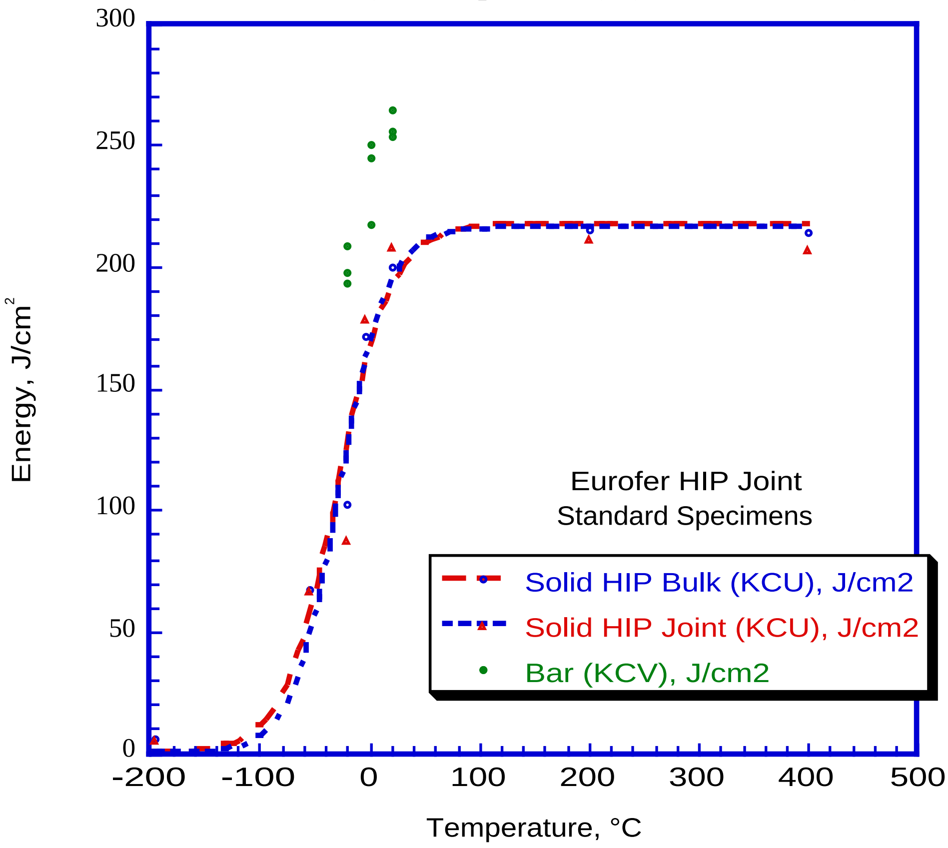

Fig. A3.S18E.6.6.4. Impact toughness of Eurofer Solid HIP product, compared with the as-received metal (Standard V and U notch specimens), (CEA data).

b. Effects of thermal aging (unirradiated)

Ductile to brittle transition temperature of Eurofer steel is increased after thermal ageing. The amount of increase is small for aging temperatures less than about 500°C. At higher temperatures the shift in DBTT becomes more important with increasing ageing time. Figures 6.6.5 and 6 show examples of such a shift.

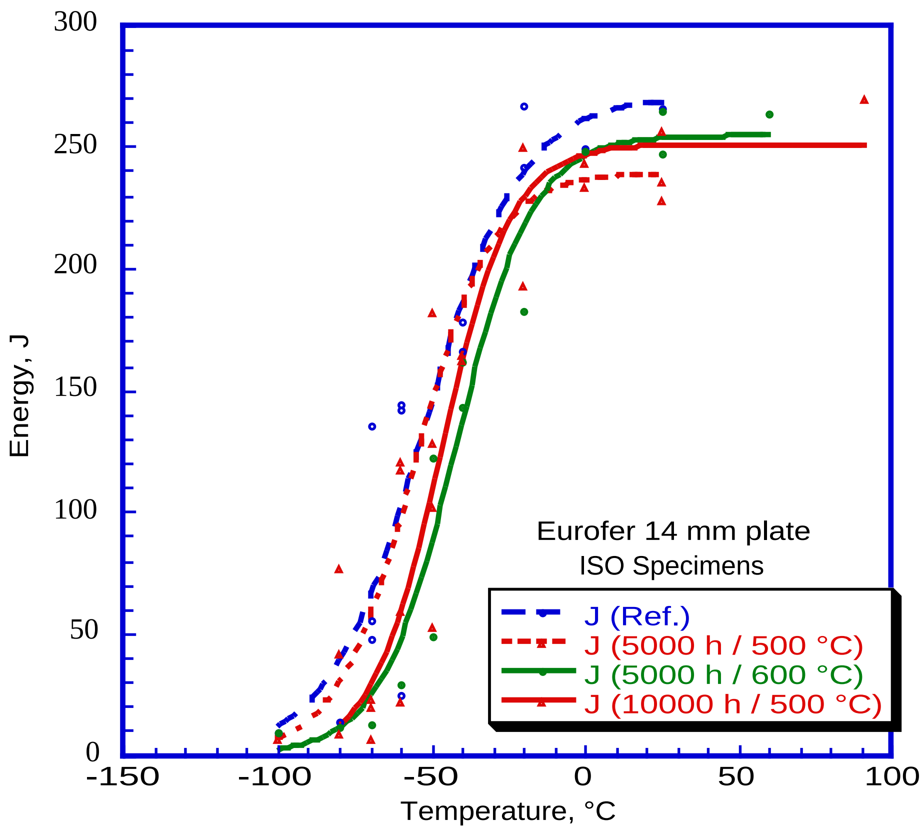

Fig. A3.S18E.6.6.5. Impact toughness of Eurofer base metal in the as-received and aged conditions, (CIEMAT data).

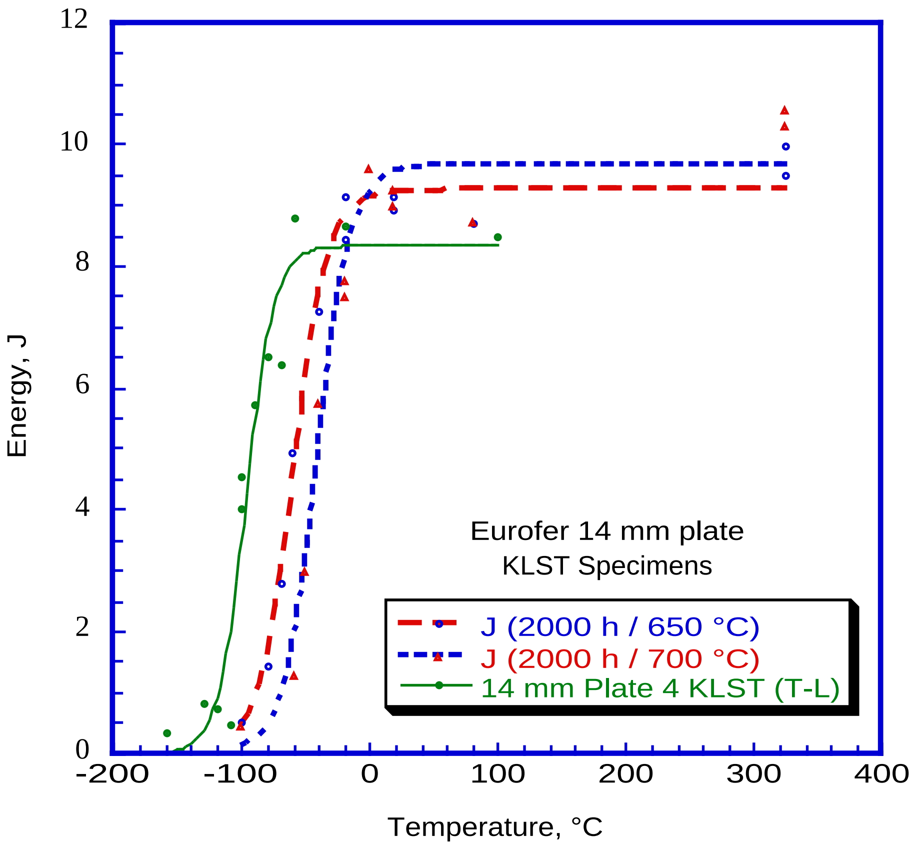

Fig. A3.S18E.6.6.6. Impact toughness of Eurofer base metal in the as-received and aged conditions, (CEA data).

c. Irradiation effects

The effect of neutron irradiation on impact toughness of Eurofer steel is by far the most important criterion regarding utilization of this steel in fusion reactors.

As a result, most of the alloy development efforts has been devoted to mitigation of this problem. This work is still in progress and not all the phenomena involved are fully understood. This is due to the fact that in addition to conventional factors affecting interpretation of this type of results we need to incorporate the effect 14 MeV neutrons and large He/dpa rations encountered in the fusion reactor. What follows below is therefore a very preliminary assessment of reported results.

Figure 6.6.6 shows effect of irradiation at 300°C on Charpy impact toughness of Eurofer steel at a very low dose. In this figure specimens are ISO type.

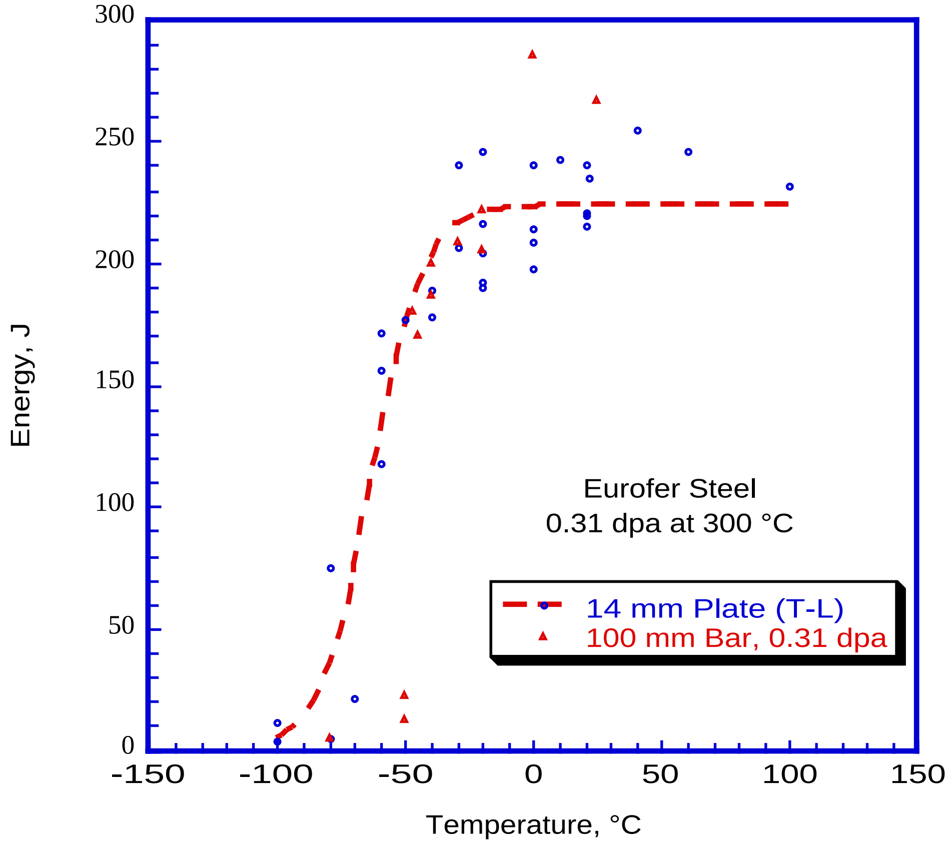

Fig. A3.S18E.6.6.6. Effect of irradiation on impact toughness of Eurofer steel at 300 °C (SCK data).

A3.S18E.6.6.2 Fracture toughness

Minimum fracture toughness is an elastically calculated measure of fracture toughness of the material in the presence of sharp flow. Unless a higher value can be justified by tests, the minimum plane strain fracture toughness under mode I loading in a plane strain specimen, K_{IC} shall be used for K_C. Alternatively, K_{JC}, which is derived from elasto-plastic J_{IC}, may be used for K_C.

J_C is an inelastically calculated measure of the toughness of a material in presence of a sharp flaw, expressed in terms of the J-integral. Likewise, unless a higher value can be justiefied by tests, the minimum J-integral under mode I loading in a plane strain specimen, J_{IC} shall be used for J_C.

So far two types of fracture toughness results have been reported for Eurofer steel. NRG and CIEMAT have used CT specimens and SCK pre-cracked Charpy specimens. SCK results are also for irradiated specimens (0.32 dpa at 300 °C), while those of NRG are for 2.7 dpa at 60 °C. Base line properties are obtained from spare specimens and reconstituted specimens.

Figure 6.6.7 shows results reported by CIEMAT with To = - 130 °C. Here the equation describing the med. Curve is:

$$KJC\ med.\ (1T) = 30 + 70\ exp.\ (0.019\ (T\text{-}To))$$

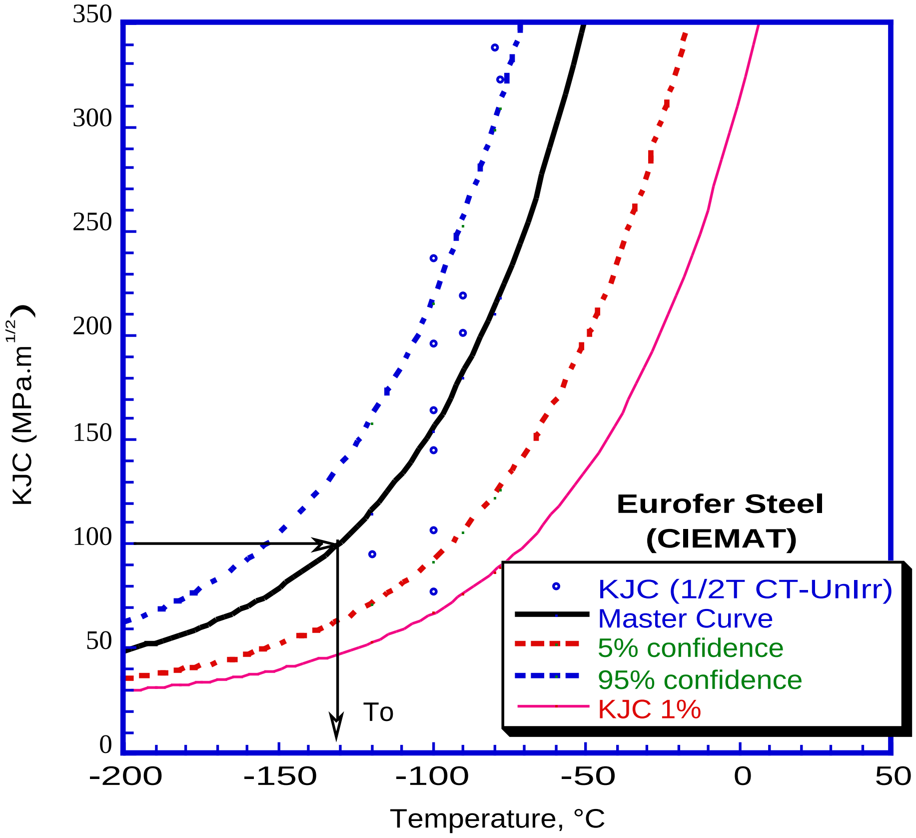

Figure A3.S18E.6.6.7. Fracture toughness data of Eurofer steel (1/2T CT specimen results), (CIEMAT data).

Figure A3.S18E.6.6.8 shows the results of fracture toughness tests performed on 5 mm and 10 mm thickness CT specimens taken from Eurofer 25 mm plate (NRG data). The results show a significant shift in To, to well above room temperature after 2.7 dap at 60 °C.

Figure A3.S18E.6.6.9 shows results obtained from tests on standard pre-cracked Charpy-V specimens. To temperature for unirradiated material is –123 °C that after exposure to 0.32 dpa at 300 °C becomes – 80 °C.

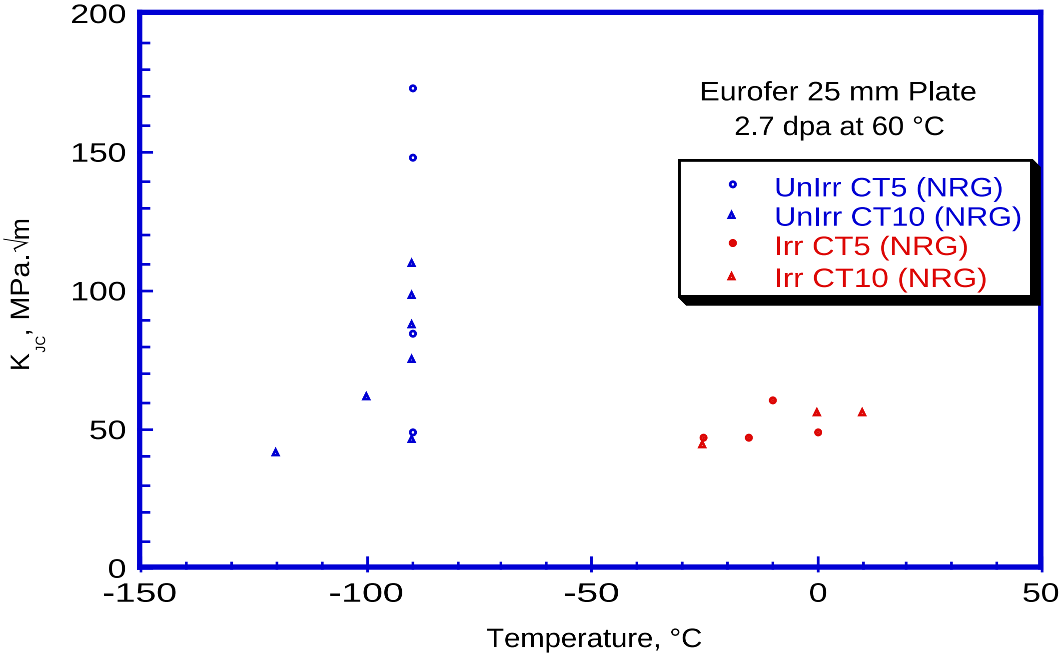

Figure A3.S18E.6.6.9. Fracture toughness data of Eurofer plate (CT specimens), (NRG data).

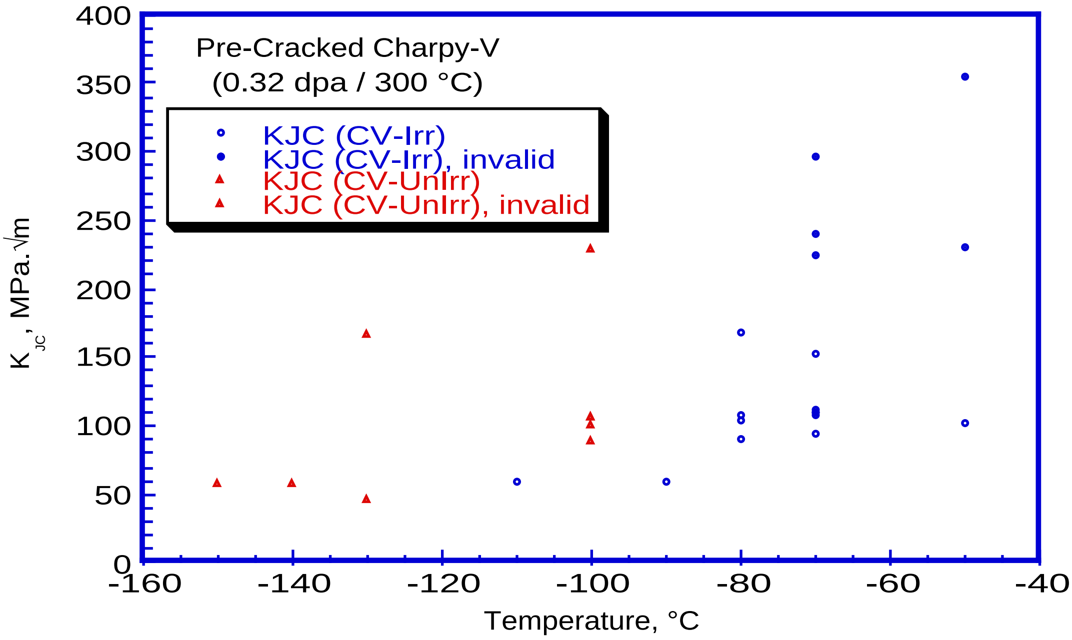

Figure A3.S18E.6.6.9. Fracture toughness data of Eurofer bar (CV specimens), (SCK data).

ANNEX 1

Products Distribution

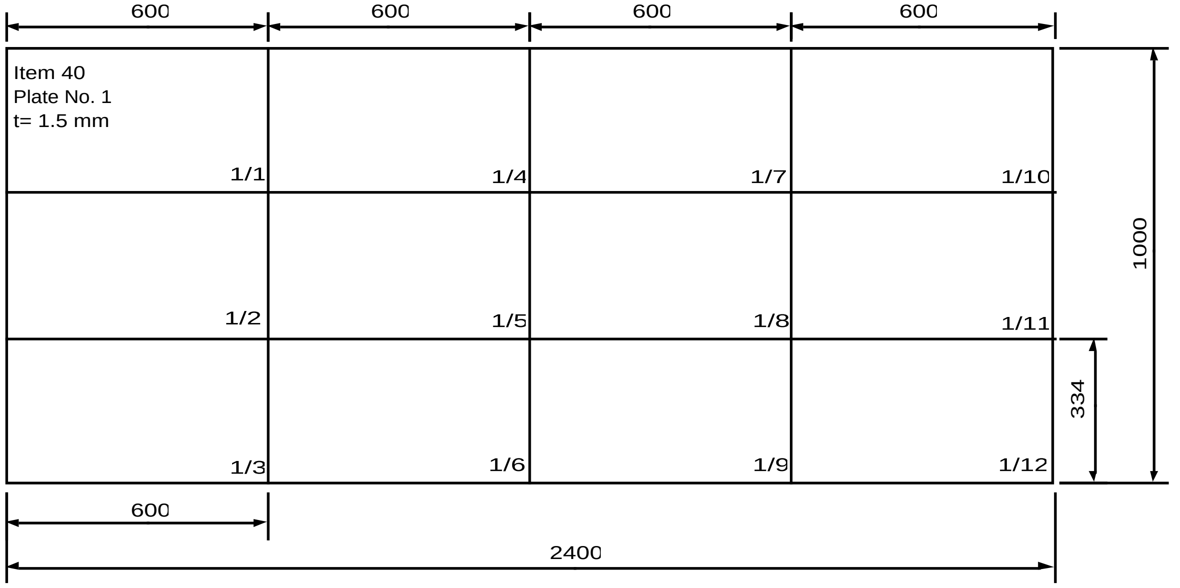

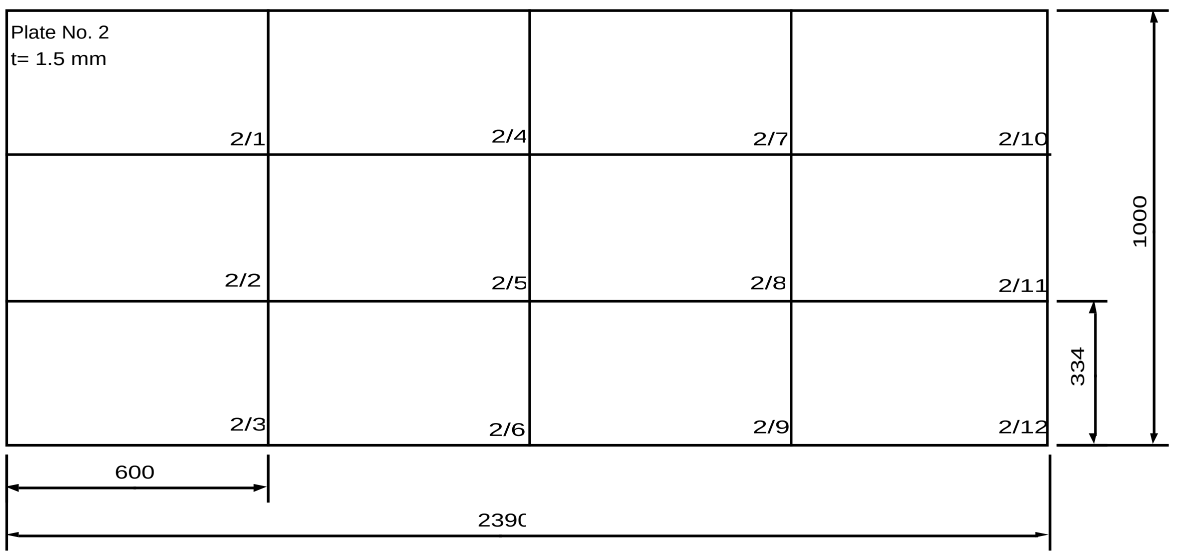

Table Annex 1.1. Item 40, Eurofer 1.5 mm plates No. 1 & 2 (Heat E83698).

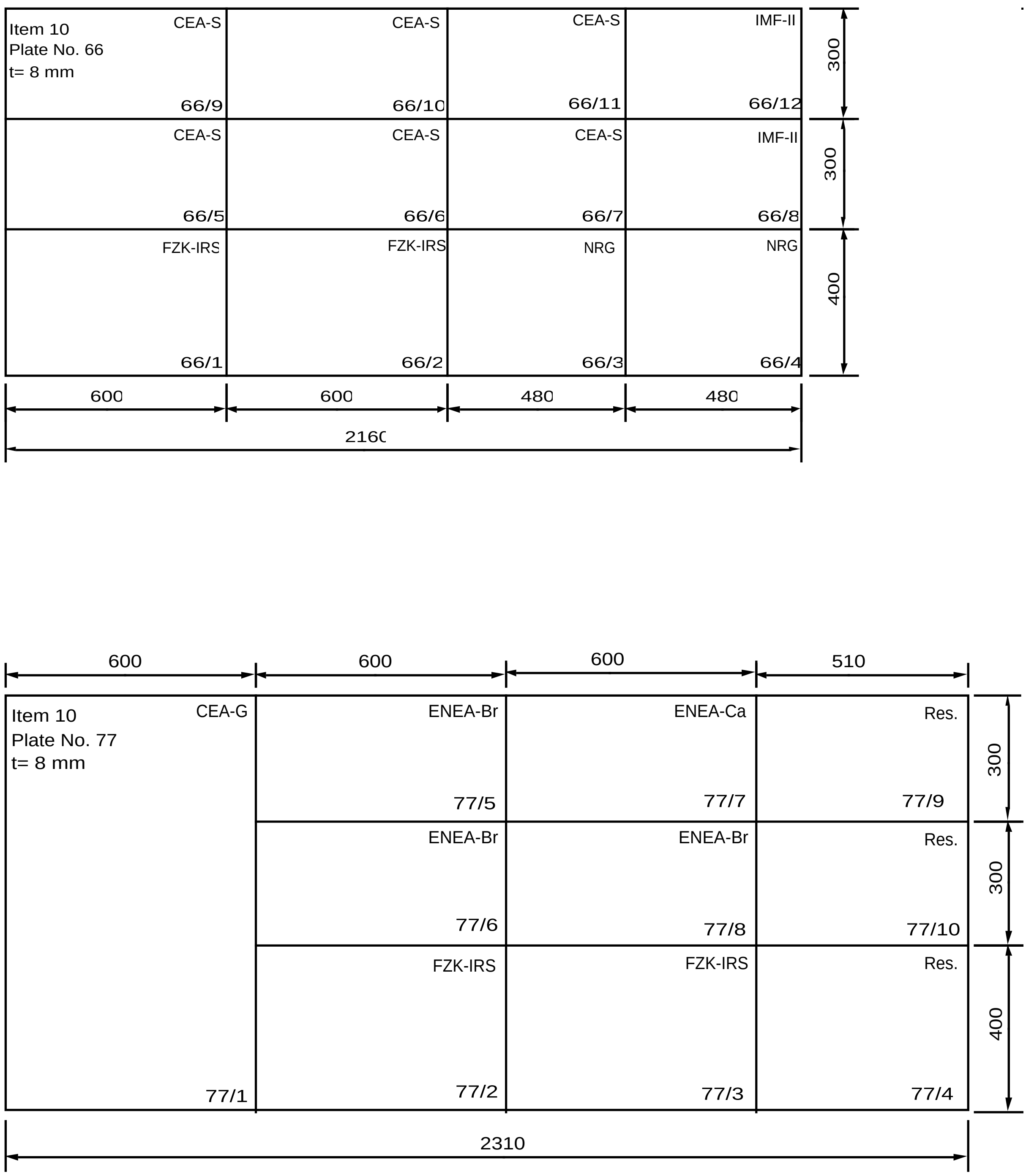

Table Annex 1.2. Item 10, Eurofer 8 mm plates No. 66 & 77 (Heat E83698).

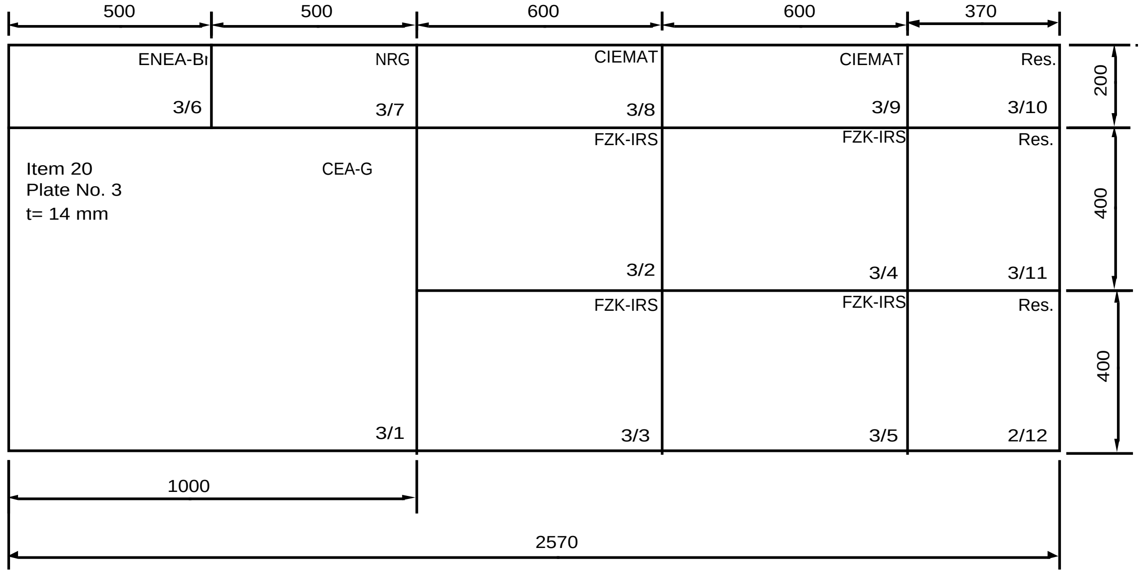

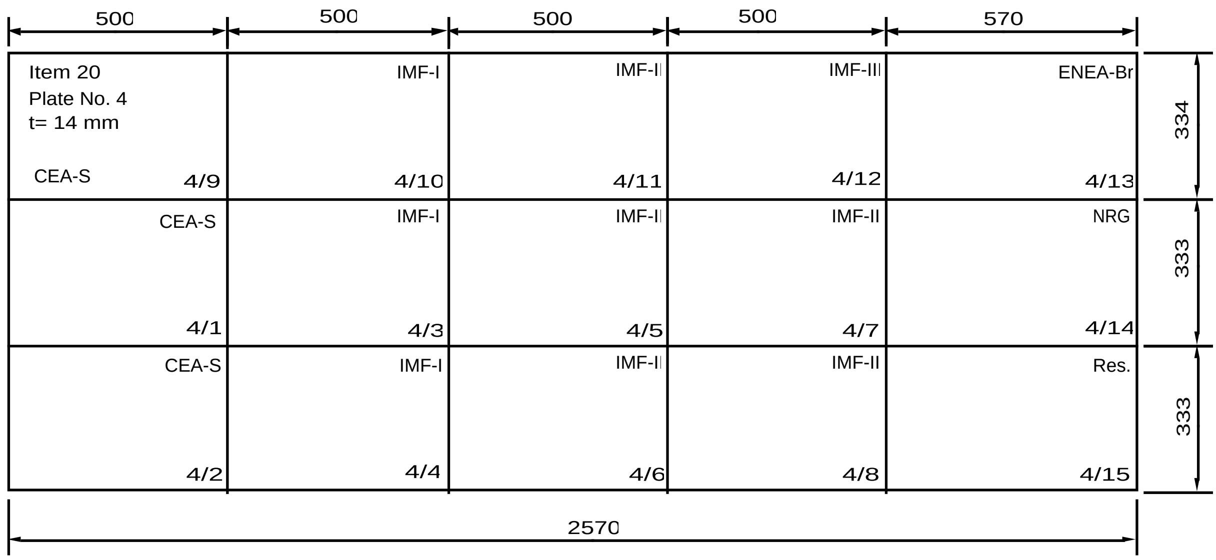

Table Annex 1.3. Item 20, Eurofer 14 mm plates No. 3 & 4 (Heat E83698).

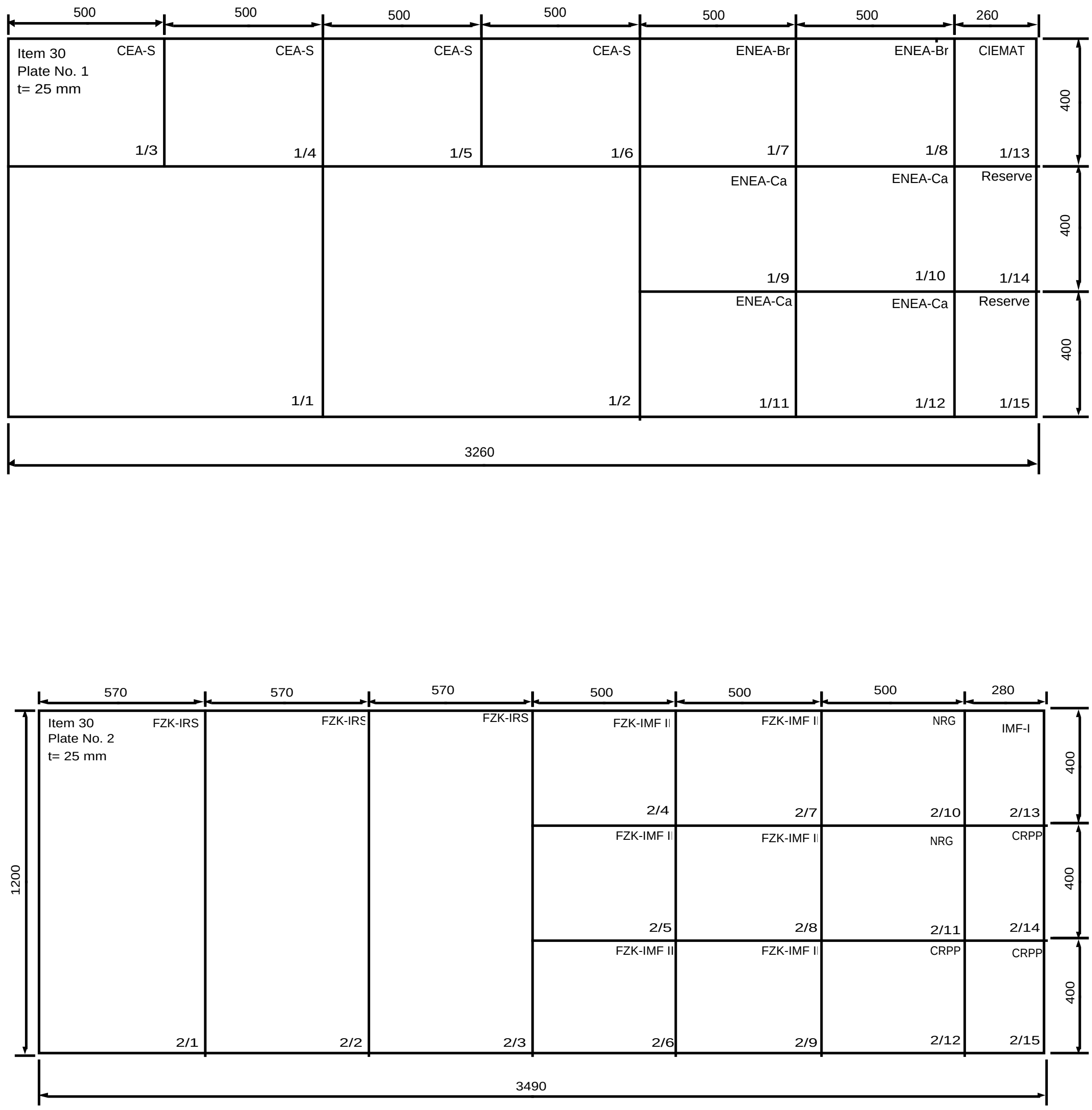

Table Annex 1.4. Item 30, Eurofer 25 mm plates No. 1 & 2 (Heat E83697).

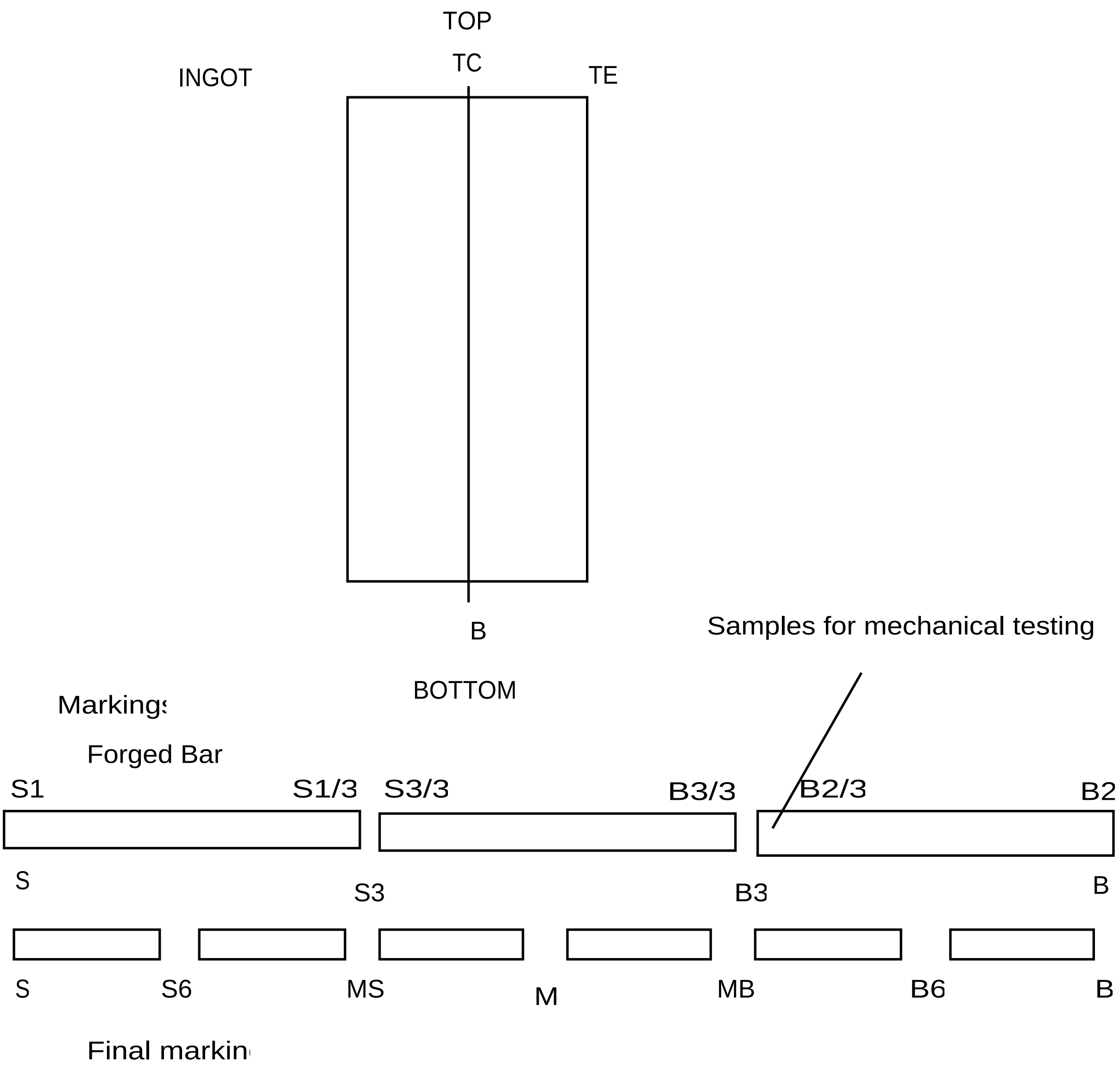

Table Annex 1.5. Final marking of 100 mm bar forging (Heat E83699).

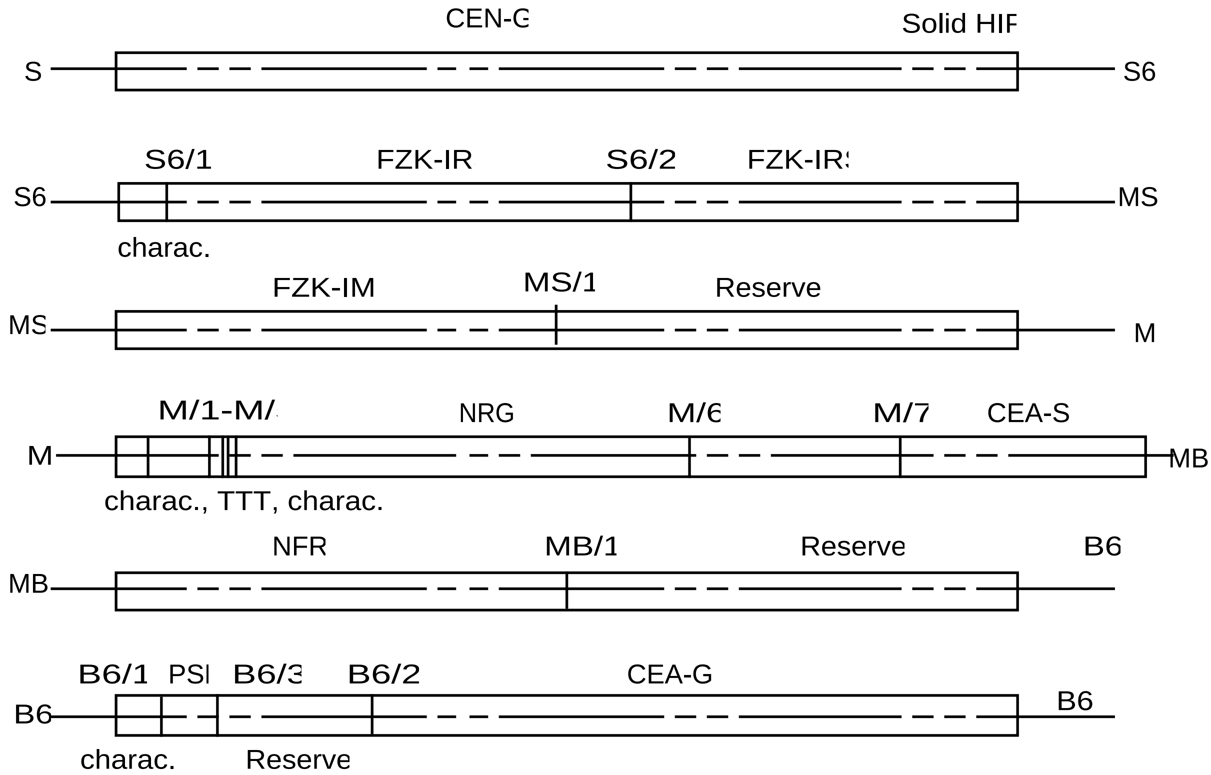

Table Annex 1.6. 100 mm bar distribution (Heat E83699).

ANNEX 2

Chemical Compositions

Notice: The data are slightly different from those supplied by Böhler and correspond to updated results supplied by R. Lindau / FZK (28/3/2001).

	Heat E83694 Forged bar 520x190mm (Inspection Cert. 029044)			25 mm Product	Heat E83697 Forged bar 520x190 (Inspection Cert. 029035)			25 mm Product
	Bottom	Top Edge	Top Center	Plate 1	Bottom	Top Edge	Top Center	Plate 2
Cr	8.77	8.89	8.76	8.87	8.82	8.95	8.93	8.93
C	0.095	0.11	0.091	0.10	0.11	0.12	0.12	0.12
Mn	0.44	0.45	0.43	0.45	0.45	0.47	0.47	0.47
P	0.005	0.005	0.005	0.005	<0.005	<0.005	<0.005	<0.005
S	0.003	0.004	0.003	0.004	0.003	0.004	0.004	0.004
V	0.19	0.2	0.19	0.2	0.19	0.20	0.20	0.20
B	< 0.001	< 0.001	< 0.001	< 0.001	< 0.001	< 0.001	< 0.001	< 0.001
N2	0.017	0.017	0.015	0.017	0.019	0.020	0.020	0.018
O2	0.0012	0.0015	0.0008	0.0009	0.0008	0.0007	0.0007	0.0012
W	1.15	1.15	1.16	1.15	1.07	1.08	1.07	1.07
Ta	0.14	0.15	0.14	0.14	0.14	0.15	0.15	0.14
Ti	0.005	0.006	0.005	0.005	0.008	0.009	0.009	0.009
Nb	0.0025	0.0025	0.0026	0.0025	0.0019	0.0020	0.0021	0.0022
Mo	0.0029	0.0031	0.0031	0.0027	0.0028	0.0019	0.0020	0.0015
Ni	0.028	0.024	0.024	0.028	0.022	0.022	0.0021	0.0022
Cu	0.0034	0.0034	0.0034	0.0035	0.0038	0.0040	0.0040	0.0036
Al	0.007	0.006	0.006	0.008	0.007	0.008	0.008	0.008
Si	0.05	0.05	0.05	0.05	0.06	0.06	0.06	0.060
Co	0.006	0.006	0.006	0.006	0.006	0.006	0.006	0.007
Sn	< 0.005	< 0.005	< 0.005	< 0.005	< 0.005	< 0.005	< 0.005	< 0.005
As	< 0.005	< 0.005	< 0.005	< 0.005	< 0.005	< 0.005	< 0.005	< 0.005
Sb	< 0.005	< 0.005	< 0.005	< 0.005	< 0.005	< 0.005	< 0.005	< 0.005
Zr	< 0.005	< 0.005	< 0.005	< 0.005	< 0.005	< 0.005	< 0.005	< 0.005
Pb	< 0.0003	< 0.0003	< 0.0003		< 0.0003	< 0.0003	< 0.0003	

Table Annex 2.1. Chemical compositions of ingots E83694 and E83697, and two 25 mm plates issued from them (tests 1F & 2F, certificate 200556).

	Heat E83698 Forged bar 520x190 mm (Inspection Certificate 029037)			14 mm Product	8 mm Product	1.5 mm Product
Elements	Bottom	Top Edge	Top Center	Plates 3, 4	Pl. 66, 77	Plates 1, 2
Cr	8.87	8.95	8.97	8.82	8.91	8.96
C	0.11	0.12	0.12	0.11	0.12	0.11
Mn	0.48	0.49	0.49	0.47	0.48	0.49
P	<0.005	<0.005	<0.005	0.005	0.005	<0.005
S	0.003	0.004	0.004	0.004	0.004	0.004
V	0.20	0.20	0.20	0.20	0.20	0.20
B	< 0.001	< 0.001	< 0.001	< 0.0010	< 0.0010	< 0.0010
N2	0.021	0.021	0.021	0.020	0.020	0.021
O2	0.0009	0.0005	0.0005	0.0010	0.0008	0.0008
W	1.08	1.08	1.08	1.09	1.08	1.08
Ta	0.14	0.15	0.15	0.13	0.14	0.14
Ti	0.006	0.006	0.006	0.005	0.006	0.006
Nb	0.0017	0.0018	0.0017	0.0016	0.0017	0.0017
Mo	<0.0010	<0.0010	<0.0010	<0.0010	<0.0010	<0.0011
Ni	0.021	0.020	0.020	0.020	0.020	0.020
Cu	0.0019	0.0020	0.0017	0.0016	0.0015	0.018
Al	0.009	0.009	0.009	0.009	0.009	0.009
Si	0.04	0.05	0.04	0.040	0.040	0.040
Co	0.006	0.006	0.006	0.006	0.006	0.006
Sn	< 0.005	< 0.005	< 0.005	< 0.005	< 0.005	< 0.005
As	< 0.005	< 0.005	< 0.005	< 0.005	< 0.005	< 0.005
Sb	< 0.005	< 0.005	< 0.005	< 0.005	< 0.005	
Zr	< 0.005	< 0.005	< 0.005	< 0.005	< 0.005	
Pb	< 0.0003	< 0.0003	< 0.0003			

Table Annex 2.2. Chemical compositions of ingot E83698, and 14, 8 and 1.5 mm plates issued from it (tests 3F, 66F and 1F, certificate 200556).

	Heat E83350 (Ingot Ø 410, Ins. Cert. 029043)			Tube 10x1	Tube 17x1.5	Tube 13.5x1.25
Elements	Bottom	Top Edge	Top Center	Plates 3, 4	Pl. 66, 77	Plates 1, 2
Cr	8.91	8.92	8.82	8.82	8.81	8.78
C	0.11	0.11	0.10	0.11	0.11	0.11
Mn	0.38	0.38	0.37	0.39	0.39	0.38
P	< 0.005	< 0.005	< 0.005	0.004	0.004	0.004
S	0.003	0.003	0.003	0.003	0.003	0.003
V	0.19	0.19	0.19	0.19	0.18	0.18
B	< 0.001	< 0.001	< 0.001	0.0008	0.0009	0.0009
N2	0.034	0.027	0.021	0.034	0.034	0.034
O2	0.0008	0.0022	0.0026	0.0049*)	0.0035*)	0.0050*)
W	1.09	1.09	1.10	1.09	1.08	1.09
Ta	0.15	0.15	0.13	0.15	0.15	0.15
Ti	0.006	0.006	0.006	0.003	0.003	0.003
Nb	< 0.001	< 0.001	< 0.001	<0.0010	<0.0010	<0.0010
Mo	0.0018	0.0012	0.0010	0.0020	0.0016	0.0017
Ni	0.023	0.020	0.021	0.022	0.020	0.020
Cu	0.0079	0.0082	0.0080	0.0080	0.0072	0.0072
Al	0.008	0.008	0.008	0.005	0.007	0.005
Si	0.05	0.05	0.05	0.05	0.05	0.05
Co	0.005	0.005	0.005	0.0030	0.0031	0.0030
Sn	< 0.005	< 0.005	< 0.005	< 0.001	< 0.001	< 0.001
As	< 0.005	< 0.005	< 0.005	< 0.001	< 0.001	< 0.001
Sb	< 0.005	< 0.005	< 0.005	< 0.005	< 0.005	< 0.005
Zr	< 0.005	< 0.005	< 0.005	< 0.001	< 0.001	< 0.001
Pb	< 0.0003	< 0.0003	< 0.0003	< 0.0003	< 0.0003	< 0.0003

Table Annex 2.3. Chemical compositions of ingot E83350, and different size tubes (mm) issued from it (certificate 0402233-2, Product analysis Böhler *0412F).

	E83699 Forged bar (Inspection Certificate 029060)			Bar
Elements	Bottom	Top Edge	Top Center	Check
Cr	8.99	8.99	8.87	8.99
C	0.12	0.12	0.12	0.12
Mn	0.44	0.44	0.42	0.44
P	< 0,005	< 0,005	0.004	< 0,005
S	0.004	0.004	0.003	0.004
V	0.19	0.19	0.19	0.19
B	< 0,001	< 0,001	< 0,0005	< 0,001
N2	0.016	0.017	0.018	0.016
O2	0.0010	0.0013	0.013	0.0010
W	1.10	1.10	1.10	1.10
Ta	0.14	0.14	0.14	0.14
Ti	0.008	0.008	0.008	0.008
Nb	< 0,001	< 0,001	< 0,001	< 0,001
Mo	< 0,001	< 0,001	< 0,001	< 0,001
Ni	0.007	0.007	0.007	0.0075
Cu	0.022	0.021	0.022	0.021
Al	0.008	0.008	0.008	0.008
Si	0.07	0.07	0.07	0.06
Co	0.004	0.004	0.004	0.005
Sn	< 0,005	< 0,005	< 0,005	< 0,005
As	< 0,005	< 0,005	< 0,005	< 0,005
Sb	< 0.005	< 0.005	< 0.005	< 0.005
Zr	< 0.005	< 0.005	< 0.005	< 0.005
Pb	< 0.0003	< 0.0003	< 0.0003	

Table Annex 2.4. Chemical compositions of ingot E83699, certificate 29060).

	E83350 Forged bar (Inspection Certificate 029101)			1 mm Wire
Elements	Bottom	Top Edge	Top Center	Check
Cr	8.91	8.82	8.92	8.93
C	0.11	0.10	0.11	0.11
Mn	0.38	0.37	0.38	0.39
P	< 0,005	< 0,005	< 0,005	< 0,005
S	0.003	0.003	0.003	0.004
V	0.19	0.19	0.19	0.19
B	< 0,001	< 0,001	< 0,001	< 0,0005
N2	0.034	0.021	0.027	0.026
O2	0.0008	0.0026	0.0022	0.0018
W	1.09	1.10	1.09	1.09
Ta	0.15	0.13	0.15	0.14
Ti	0.006	0.006	0.006	0.006
Nb	< 0,001	< 0,001	< 0,001	< 0,001
Mo	0.0018	0.0010	0.0012	0.0010
Ni	0.023	0.021	0.020	0.020
Cu	0.0079	0.0080	0.0082	0.074
Al	0.008	0.008	0.008	0.007
Si	0.05	0.05	0.05	0.05
Co	0.005	0.005	0.005	0.005
Sn	< 0,005	< 0,005	< 0,005	< 0,005
As	< 0,005	< 0,005	< 0,005	< 0,005
Sb	< 0.005	< 0.005	< 0.005	< 0.005
Zr	< 0.005	< 0.005	< 0.005	< 0.005
Pb	< 0.0003	< 0.0003	< 0.0003	

Table Annex 2.5. Chemical compositions of ingot E83550, certificate 29101).

ANNEX 3

Hardness and Microstructure

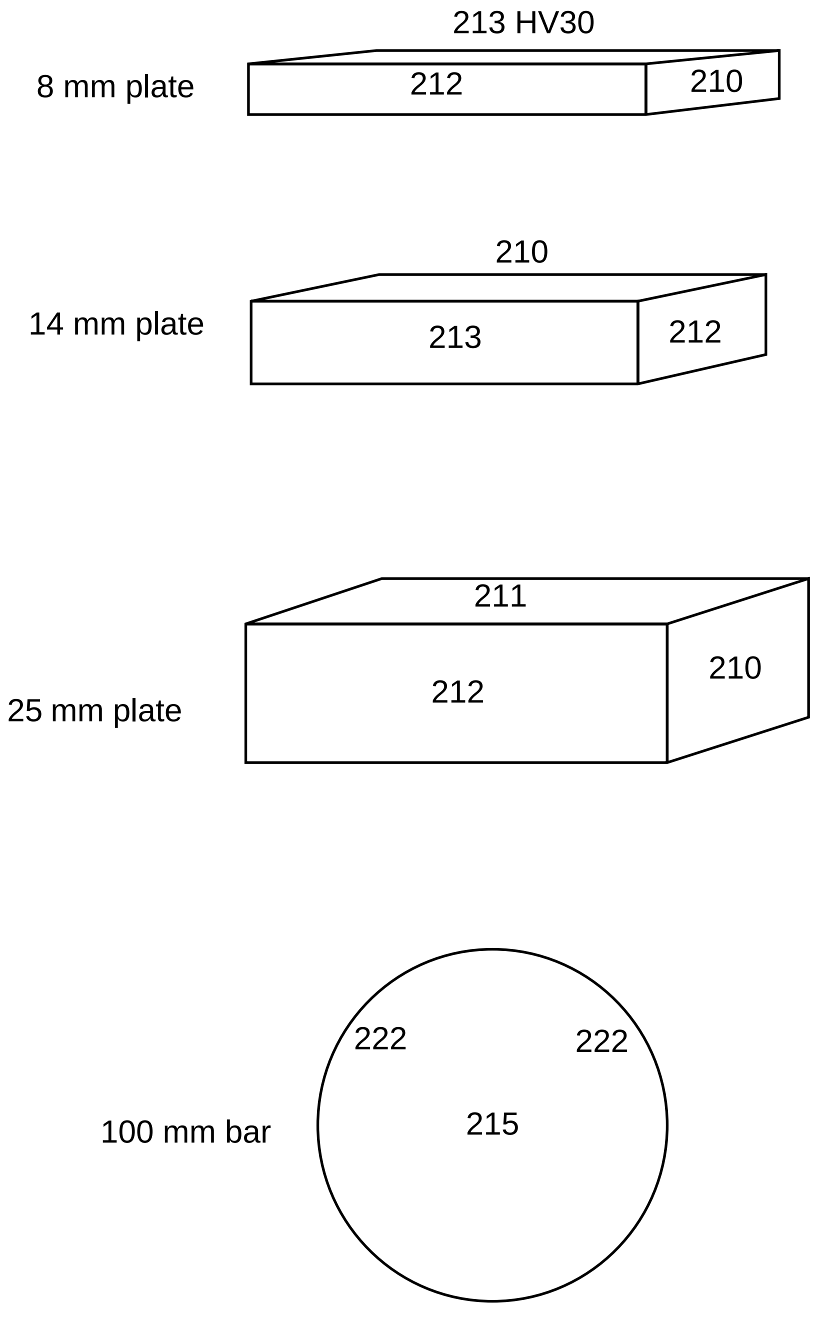

Figure Annex 3.1. Hardness of Eurofer products (NRG data).

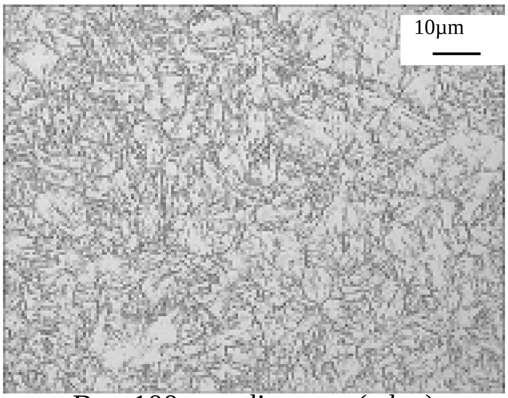

Bar, 100 mm diameter (edge)

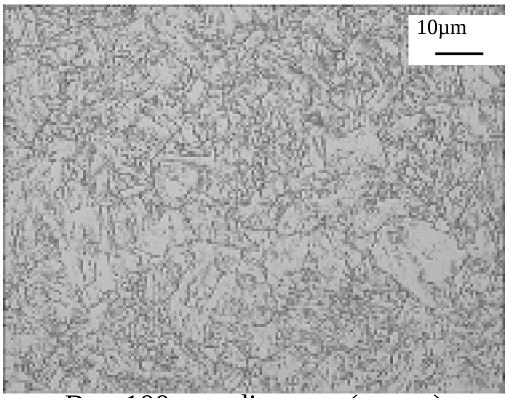

Bar, 100 mm diameter (centre)

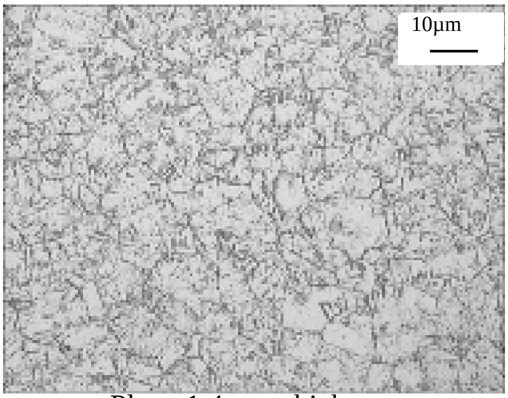

Plate, 1.4 mm thickness

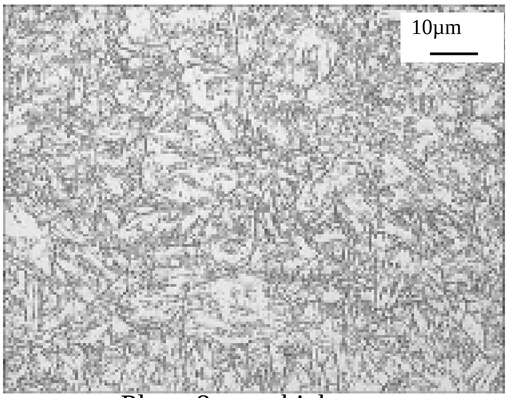

Plate, 8 mm thickness

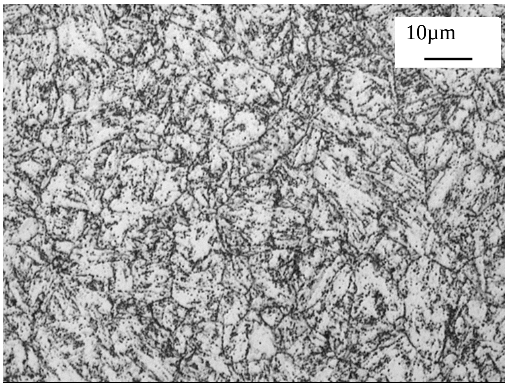

Plate, 14 mm thickness

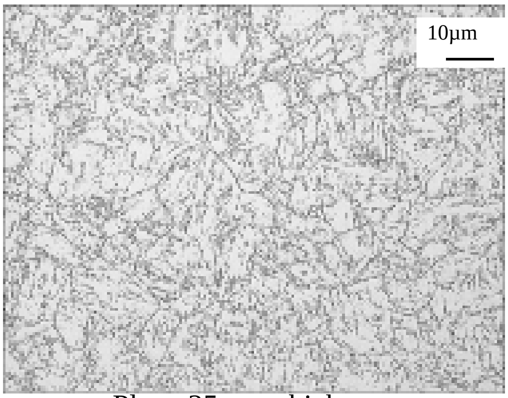

Plate, 25 mm thickness

Figure Annex 3.1. Optical micrographs of the as-received Eurofer97 products Observations on the cross-sections parallel to the rolling direction (CEA data).

ANNEX 4

HIP Products

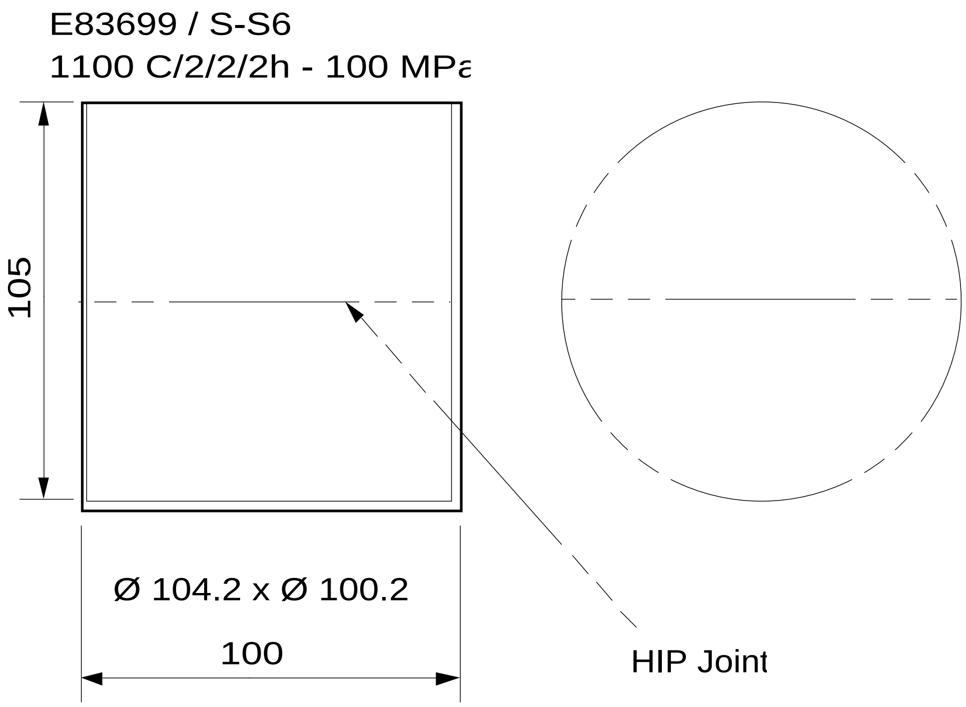

Figure Annex 4.1. Eurofer solid HIP joint manufacturing (CEA data).

ANNEX 5

Evolution of maximum stress in tension and in compression during fatigue.

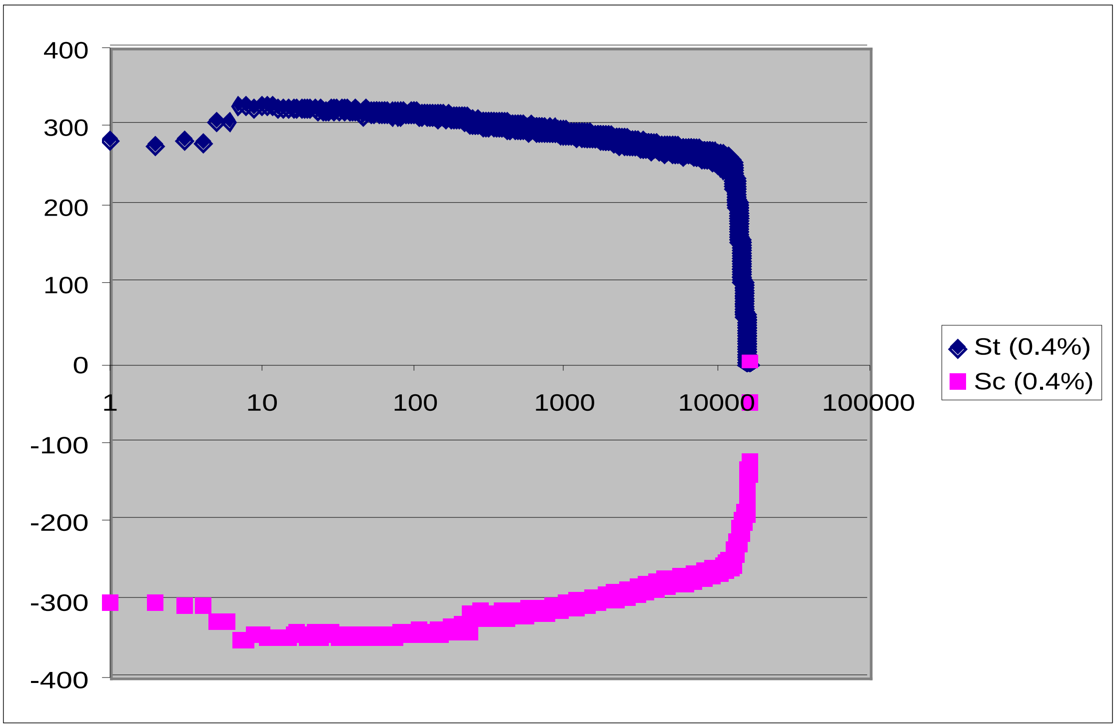

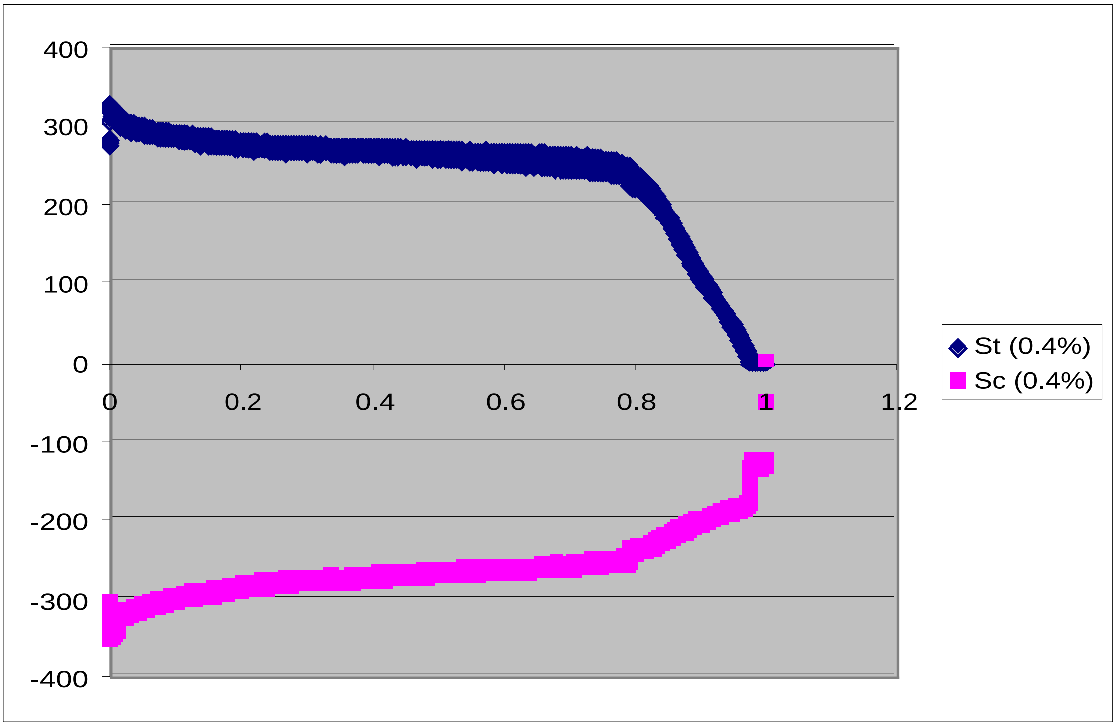

Figure Annex 5.1. Variation of maximum stress in tension and in compression versus number of fatigue cycles (CIEMAT data, Eurofer Plate, 500 °C, $\Delta\varepsilon t$ = 0.4%).

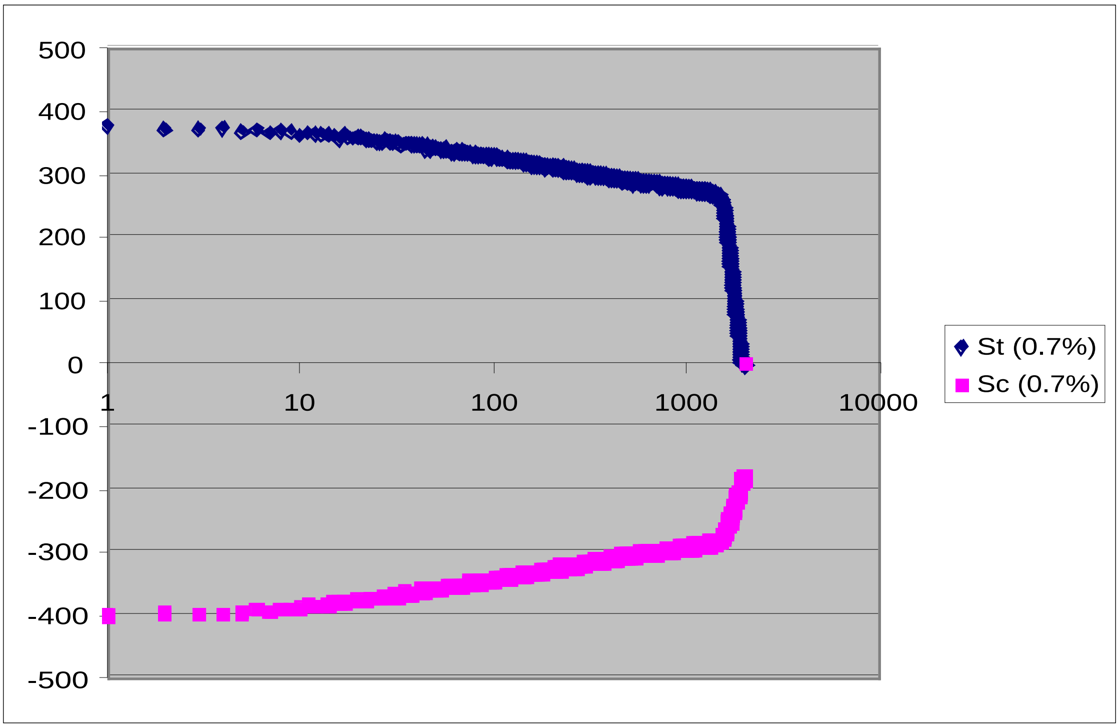

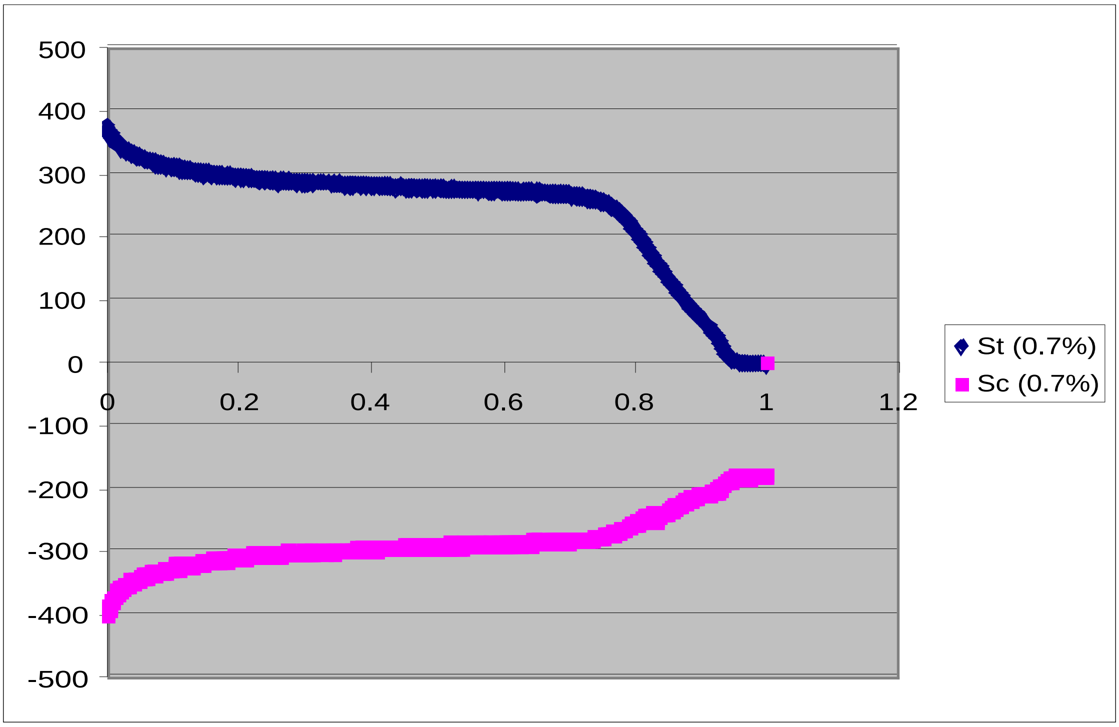

Figure Annex 5.2. Variation of maximum stress in tension and in compression versus number of fatigue cycles (CIEMAT data, Eurofer Plate, 500 °C, Δεt = 0.7%).

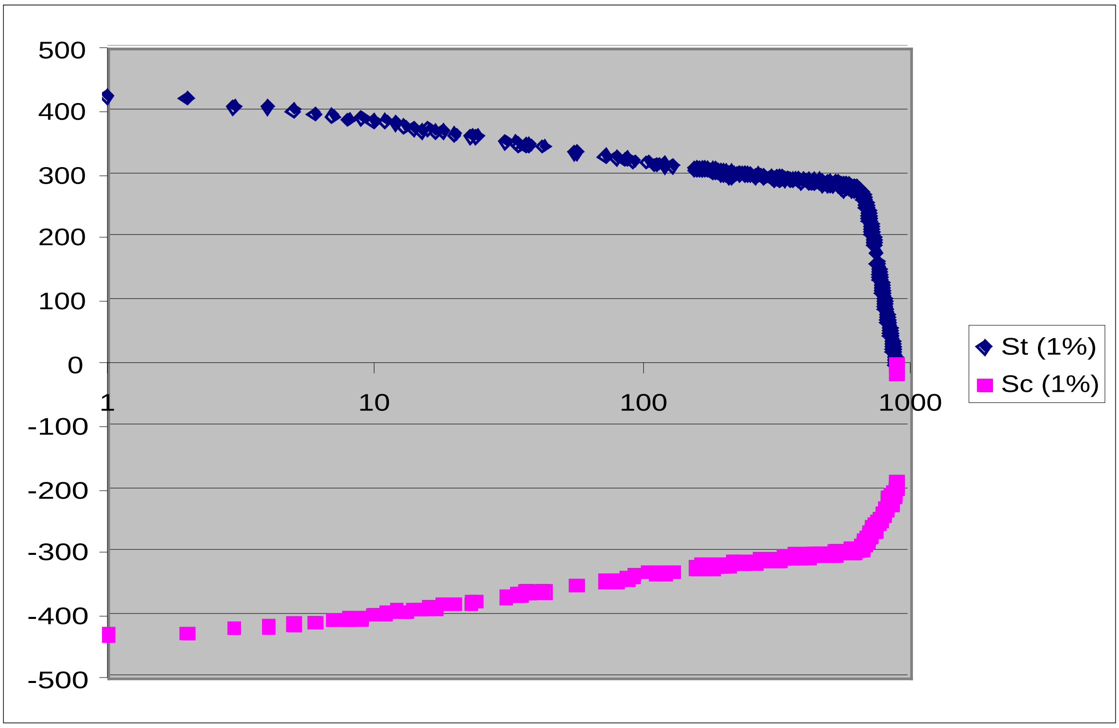

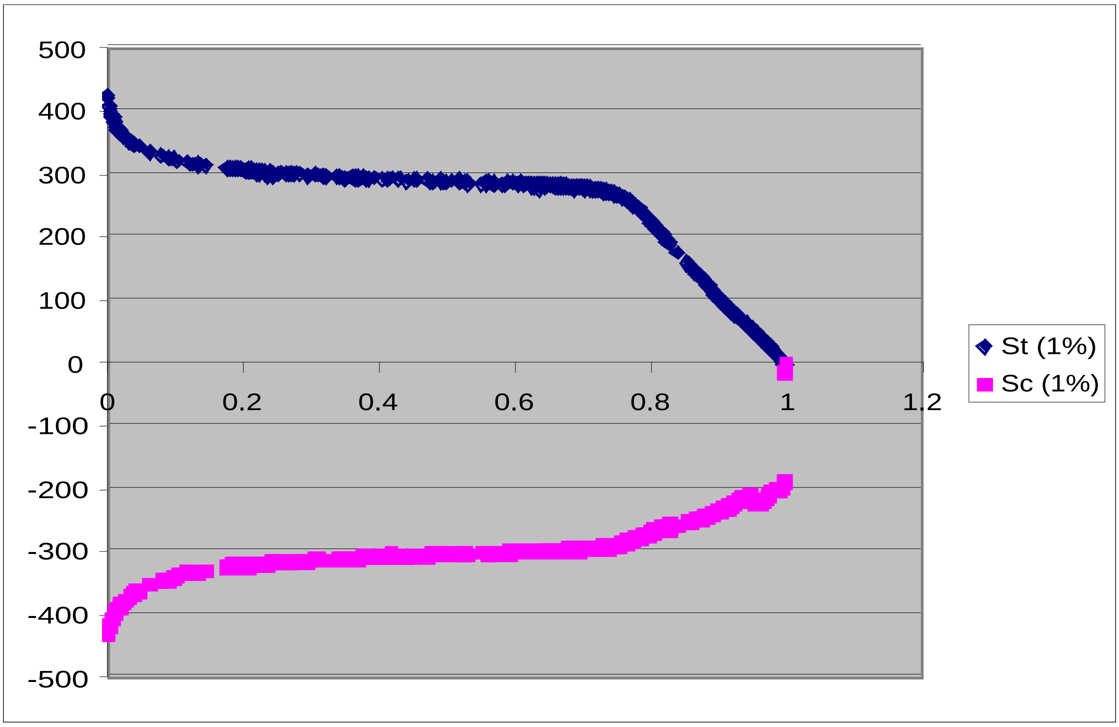

Figure Annex 5.3. Variation of maximum stress in tension and in compression versus number of fatigue cycles (CIEMAT data, Eurofer Plate, 500 °C, Δεt = 1%).

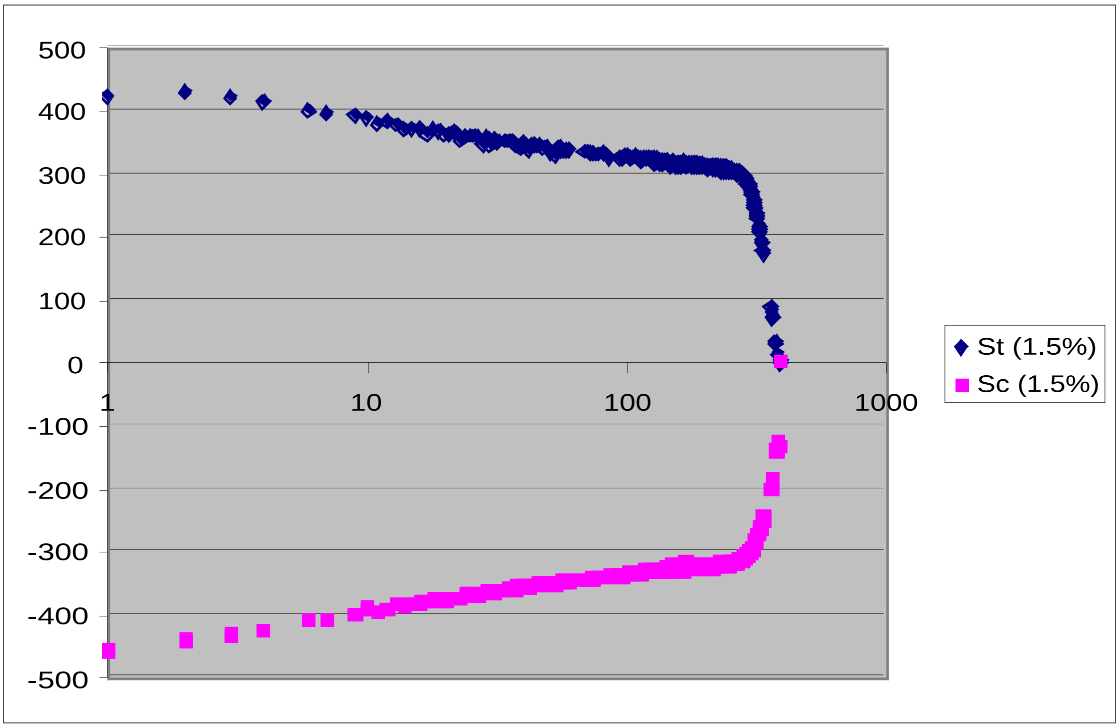

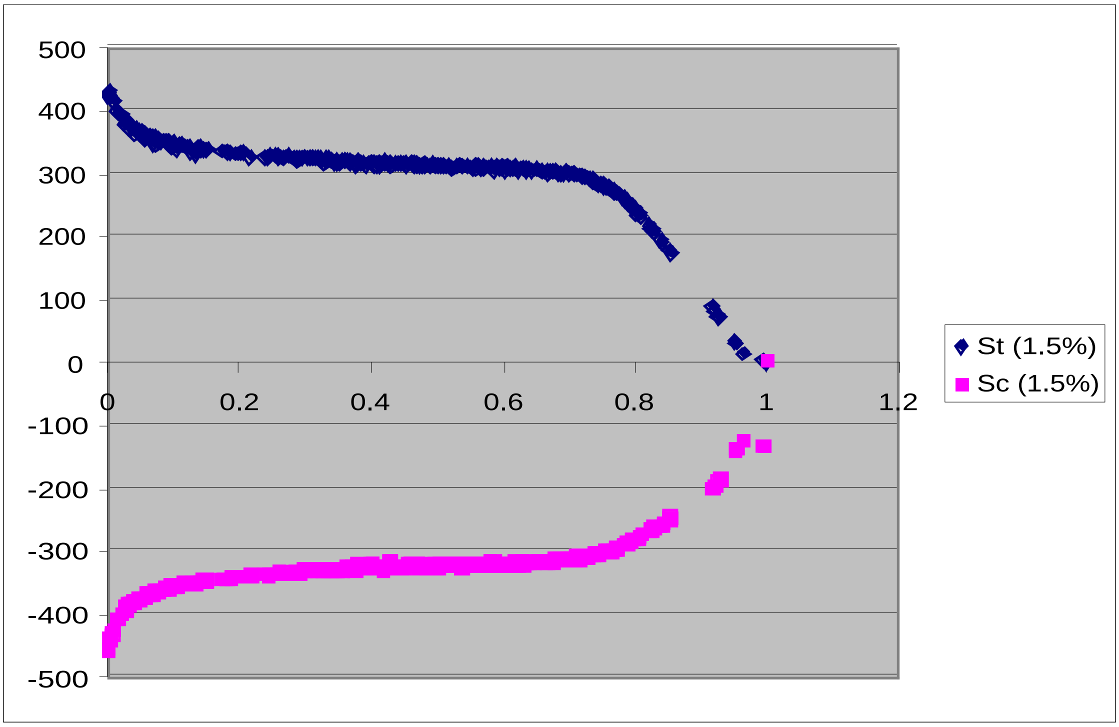

Figure Annex 5.4. Variation of maximum stress in tension and in compression versus number of fatigue cycles (CIEMAT data, Eurofer Plate, 500 °C, Δεt = 1.5%).